Fault Diagnosis and Localization of Solar Photovoltaic Fed Cascaded H-Bridge Multi-Level Inverter

By

Iqra Ashfaq

00000364098

Supervisor

Dr. Azhar Ul Haq

Department of Electrical Engineering

A thesis submitted in partial fulfillment of the requirements for the degree of MS 21 (EE)

In

CEME,

National University of Sciences and Technology (NUST),

Islamabad, Pakistan.

(August 2024)

THESIS ACCEPTANCE CERTIFICATE

It is certified that final copy of MS/MPhil thesis written by Ms. Iqra Ashfaq (Registration No. 00000364098) Entry-2021, of (College of E&ME) has been vetted by the undersigned, found complete in all respects as per NUST Statutes/Regulations, is free of plagiarism, errors, and mistake and is accepted as partial fulfillment for award of MS degree. It is further certified that necessary amendments as pointed out by GEC member of the scholar have also been incorporated in the said thesis.

Signature: ______________________

Name of Supervisor Dr. Azhar Ul Haq

Date: 15 - Aug. 2024

Signature (HoD): ______________________

Dr. Qasim Umar Khan

Date: 15 - Aug. 2024

Signature (Dean): ______________________

Brig Dr. Nasir Rashid

Date: 15 AUG 2024

Dedication

This thesis is dedicated to all the deserving children who lack access to quality education, with an emphasis on young girls.

Acknowledgments

Glory be to Allah (S.W.A), the Creator and Sustainer of the Universe. He alone has the power to honor whom He pleases and to humble whom He pleases. Truly, nothing can happen without His will. From the day I arrived at NUST until the day of my departure, He was the One who blessed me, opened doors for me, and guided me on the path to success. No words can adequately express my gratitude for His countless blessings throughout my research journey.

I express my profound gratitude to Dr. Azhar Ul Haq for his invaluable guidance, patience, and encouragement throughout the research process. This thesis would not have taken this shape without his constructive criticism and insight. My earnest gratitude goes to my cosupervisor Dr. Zaki Uddin, whose immense support and expertise contributed in the making of this thesis. I also thank the members of the Graduate Examination Committee (GEC), namely Dr. Salman Qadir and Dr. Touseef Iqbal, who supported me with their valuable feedback and recommendations.

I am thankful to my mother for being the backbone of my strength and inspiration through her love, prayers, and sacrifices. Finally, I would like to thank my eldest sister for the support, belief in me, and constant encouragement at each step of this research journey. Their support and belief in me have been invaluable, and I am deeply appreciative of their contributions toward my academic journey.

Iqra Ashfaq

Abstract

This research introduces a deep learning approach for detecting and localizing switch faults in Photovoltaic (PV) systems, specifically targeting PV fed cascaded H-bridge 5-level inverters. The study's primary focus is on identifying both single short circuit faults and up to two open switch faults, aiming to enhance the reliability of this inverter. The research utilizes a Residual Network (ResNet) architecture with residual connections to effectively identify and localize faults. Extensive testing across 48 unique fault classes and one non fault case demonstrated the model's robustness, achieving an accuracy of 92% at -20 dB noise, approximately 94% at -10 dB and 0 dB, and around 95% at 10 dB and 20 dB. The model was trained using NVIDIA A100 GPU. This research highlights the development of a real-time fault detection system capable of operating under multiple modulation indices, ranging from 0.55 to 1, in the presence of both single and double switch faults. By incorporating noise signals, the study addresses practical challenges in solar inverter operations and advances the methodology for detection of fault in PV systems. The results underscore the potential of proposed methodology to markedly improve upon the reliability and performance of renewable energy technologies, marking a progressive step in fault detection for solar energy systems.

Table of Contents

List of Figures

List of Tables

List of Abbreviations

Abbreviations

CHBMLIs	Cascaded H-Bridge Multi-Level Inverters
MLIs	Multi-Level Inverters
PV	Photovoltaic
FCN	Fully Convolutional Network
CNN	Convolutional Neural Network
LSTM	Long Short Term Memory
ResNet	Residual Network
ML	Machine Learning
AI	Artificial Intelligence
AC	Alternating Current
DC	Direct Current
NPC	Neutral Point Clamped
FC	Flying Capacitor
WGN	White Gaussian Noise
MPPT	Maximum Power Point Tracking
MPP	Maximum Power Point
THD	Total Harmonic Distortion
CHB	Cascaded H-bridge

CHAPTER 1

Introduction

This thesis delves into the multifaceted process of fault detection in solar inverters, highlighting its significance in maintaining system safety and efficiency. As reliance on solar energy shifts from convenience to necessity, the continuous operation of PV systems becomes crucial. Early fault detection is vital to prevent catastrophic failures, electrical risks, and system breakdowns that pose dangers to human health and system integrity. Inverters are the core of solar power systems, and any performance deviation can lead to reduced energy efficiency and output. Rapid identification and rectification of faults are essential to keep solar installations running at maximum efficiency.

Beyond performance and safety, fault detection techniques serve a preventive role, protecting the system from extensive and costly damage caused by prolonged undetected issues. This not only preserves the health of the solar inverter but also safeguards the broader investment in solar infrastructure. Effective fault detection underpins good maintenance and troubleshooting practices, enabling targeted and efficient interventions that reduce downtime and repair costs. This approach provides maintenance teams with actionable insights for swift issue resolution. Furthermore, prompt fault detection ensures grid stability by preventing solar power integration from causing disruptions or variations that could impact the wider electrical grid.

The thesis is structured into several chapters, beginning with an introduction to the fundamental principles of PV systems and multilevel inverters. It then reviews existing methodologies and technologies for fault detection, from traditional techniques to advanced machine learning approaches. Subsequent chapters present the research methodology, results, culminating in a discussion of findings and their implications. The study emphasizes the importance of fault detection techniques for enhancing the reliability and efficiency of solar power systems. This research contributes to the development of robust fault detection systems that ensure the longevity and stability of solar energy infrastructure.

1.1 Background

Solar energy systems have become a cornerstone of sustainable energy production, utilizing PV panels for the conversion of solar radiation into electricity. These systems are composed of several interconnected components, including PV panels, electrical wiring, regulation and conversion systems, and inverters. In particular, inverters play a vital role for the conversion of DC output from solar panels into AC power, which is suitable for use in most electrical applications.

While solar energy systems offer numerous benefits, they are not immune to faults and failures, which can significantly impact their performance and reliability. Inverters mostly have faults of open circuit and short circuit; these mainly occur in the H-bridge inverter and switches of the DC-DC converter. These types of faults can disturb the flow of power and, in critical situations, also affect the whole-system stability. Detecting and diagnosing these faults are crucial to ensure continuity in power generation, avoiding other system component damages, and most importantly, for maximizing system efficiency.

Open switch faults are a situation in which some switches of the inverter fail to conduct properly for a duration of time required. Conversely, short-circuit faults are usually unintended low-resistance connections between two points that allow excessive current flow leading to heating and damage. Any type of fault may result from various causes such as manufacturing defects, aging, or environmental stresses.

To diagnosis open and short circuit faults for H-bridge inverters is a difficult task. Very high complexity, large possibilities of switching states, and power semiconductor devices are the main causes for detecting complications. Traditional fault diagnosis methods often depend on complex mathematical modeling and are time-consuming, requiring extensive expert knowledge that may not cover all the possible cases of fault occurrence. Therefore, there is a growing need for more advanced fault detection techniques in real time with dependability and efficiency for detecting various kinds of faults, including open and short-circuit faults.

A detection algorithm is designed in this work for fault diagnosis, which is primarily aimed at locating and diagnosing open and short circuit faults in H-bridge inverters and DC-DC converter switches of a PV system. The algorithm have high detection accuracy, automatically diagnose and localize faults using techniques of deep learning. This research will enable better reliability and safety of the solar system, proactive maintenance, and troubleshooting to support sustainable energy production.

1.2 Problem statement

In renewable energy systems, especially Cascaded H-Bridge Multi-Level Inverters (CHBMLIs) fed by solar energy, achieving high-quality and efficient AC power is crucial. These systems are essential for reducing harmonic distortion and meeting the strict standards required for grid integration of solar power. However, their complexity introduces significant challenges, particularly in detecting faults like open and short circuits in both the inverters and DC-DC converters. Such faults can greatly compromise the stability and in turn, the reliability of the system.

One of the major issues in fault detection for 5-level Cascaded H-bridge (CHB) inverters and DC-DC converter switches is the inherent variability in solar energy inputs. This variability makes it difficult to accurately identify faults, as the systems' complex designs involve numerous switches configured to achieve higher voltage levels and better waveform quality. Each switch's condition must be meticulously monitored to prevent disturbances that could damage the inverter, DC-DC converter, or the connected grid systems. If not properly addressed, faults such as open or short circuits can lead to severe problems, including excess current flow, overheating, and potentially catastrophic system failures. The main challenge is to distinguish between normal operational fluctuations and actual fault conditions, which many existing detection methods struggle to do.

To address these issues, advancements in fault detection frameworks for solar-fed 5-level CHB inverters and DC-DC converters are needed. This research aims to enhance the robustness, reliability, and real-time performance of fault detection systems, focusing on increasing system uptime and operational efficiency. Quick and accurate detection of fault is key to minimize downtime and maximize energy production. Properly identifying open and short-circuit faults is critical for maintaining overall system stability, which is key to integrating renewable energy sources into mainstream power grids.

This study is directed towards developing cutting-edge fault detection technologies for CHB inverters and DC-DC converters, making renewable energy systems more robust and efficient. By overcoming fault detection challenges in these systems, this research will enhance the reliability and sustainability of electricity generation from solar power, contributing to a more stable and dependable energy infrastructure.

1.3 Objectives

The primary objectives of this research are:

- Detecting and localizing open and short circuit faults.
- Proposing a deep learning method that achieves high fault detection and localization accuracy.
- Reducing time and cost of manual fault diagnosis.
- Improving reliability and robustness against different modulation indexes.

The main objective is to implement improvements in the efficiency and reliability of solar power systems by detecting high-level faults in the local control system. One of the main objectives is to develop a system for diagnosing and finding solar inverter faults. This is a critical aspect as it ensures that errors are not only detected but also specific, enabling quick response and correction.

To achieve this goal, this research aims to harness the prowess of deep learning methods. By proposing and implementing a deep learning method, this research aims to achieve the accuracy of fault detection and localization. Deep learning, with the ability to analyse complex and heterogeneous data, provides the ability to increment the accuracy and reliability of detecting faults in the inverters, and thus reduce the risk of incorrect detection if it is a false alarm. Another objective of this study is time and cost-effectiveness. By using advanced fault detection methods, this research aims towards reduction of time and cost of manual fault detection. Not only does this make maintenance and troubleshooting easier, but it also makes solar power installations more economical by reducing operating and maintenance expenses.

1.4 Contributions

This research addresses critical challenges in the fault detection of open and short-circuit switches in 5-level CHB inverters, powered by solar energy. The contributions aim to bolster the robustness, reliability, and real-time performance of fault detection systems within these complex inverter configurations, including both the inverters and associated DC-DC converters. By focusing on these areas, we seek to develop advanced detection techniques that can more effectively manage the inherent complexities and variability of solar energy systems, thereby improving overall system stability and efficiency.

1. **Comprehensive Fault Detection Framework for 5-Level H-Bridge Multi Level Inverters**: Multi-Level Inverters (MLIs), more so of 5-level H-Bridge configurations, play a very critical role in developing superior quality AC outputs that carry low harmonic distortion in renewable energy systems. The fault detection of these systems is difficult because of their complexity and variability in power sources. Thus, a fault detection structure has been designed for the robustness of the 5-level CHB inverter in compliance with all probable configurations of the power sources:

   - *Both Bridges Supported by Solar*: Compensates for the variability and intermittency of solar energy.
   - *Upper Bridge Supported by DC and Lower by Solar*: Stability is first provided to the DC sources, while reliability is improved with the variability of solar energy.
   - *Lower bridge is supported by DC and the upper by solar*: It is a hybrid approach with an application in equal power variability management and improving system reliability.

2. **Single and Double Switch Fault Detection**: Accurate detection of single and double switch faults is a must to avoid instability in the system or cascading failure. Existing methods invariably have some sort of shortcomings in classifying of these types of faults. Our model ensures the smooth and continuous operation of an inverter for the uninterrupted power supply, since it can detect single short circuit fault and upto two open switch faults with high reliability.

3. **Robustness Across Different Modulation Indexes**: The modulation index greatly affects the inverter's performance. Active fault detection should be viable under a spread of different modulation indexes so that this method does not lose its viability over different working conditions. We collected and analyzed data for different modulation indices, as this will increase the model's capacity to detect the faults with reliability across different situations. This ensures robustness of the fault detection system and its implementability with regards to real-world settings.

4. **Simulation of Real-Time Scenarios by White Gaussian Noise**: The conditions in real life

are always noisy and uncertain, making the environment very stochastic. The addition of white Gaussian noise into our data thus simulates these real-time scenarios. Hence a fault detection model is made robust. This ensures the model's practical and noisy accuracy and reliability; it separates real faults from anomalies caused by noise.

1.5 Applications areas

Techniques for open and short switch fault detection applied to CHBMLIs fed with solar energy are crucial for enhancing the reliability, efficiency, and service life of solar power generation and its grid integration. Here are detailed insights into the application areas:

1. **Enhanced reliability of solar power systems:**

    - Continuous operation: The fault detection mechanisms protect solar power systems from short and open switch faults and other disturbances, ensuring that electricity generation is continuous with minimal reduction.

    - Maintenance Schedule Optimization: Early fault detection supports the ability to proactively schedule maintenance compared to a calendar- or usage-hour-based schedule. This proactive approach ensures that the overall reliability and availability are maximized to meet grid demand and stability requirements.

2. **Grid stability and power quality improvement**:

    - Grid disturbance management: The fault-ride-through-capable inverters smooth the grid disturbances caused by faulty switches, with consumers continually obtaining stable energy even when there is a fault.

    - Harmonic reduction: Harmonics are reduced with fault detection systems, enhancing power quality since the inverters provide a clean sine wave output without any electrical noise or interference.

3. **Optimized energy harvesting and efficiency**:

    - Maximization of energy yield: Fault detection enhances energy harvesting from solar panels to maximize energy yield and system profitability.

- Efficient conversion of energy: Fault-tolerant inverters are efficient in converting energy, minimize the amount of energy lost during DC to AC conversion, and are therefore important for extracting as much as possible from any renewable energy system

4. **Cost savings and operational efficiency**:

   - Low maintenance costs: Solar power fault detection systems lower maintenance occurrences dramatically, thus minimizing the cost involved in operation downtime.
   - Real-time optimization: Quick detection and rectification of errors are undertaken to ensure maximum performance of solar PV systems with minimum opportunities lost.

5. **Safety and compliance**:

   - Safety assurance: Fault detection systems increase safety in the system by averting hazards caused by inverter malfunctions, hence proving conformity to all the safety regulations of solar power installations.
   - Reliable compliance: Reliability of the fault detection system ensures compliance with grid codes and operating standards, building trust in utilities and regulatory authorities.

6. **Integration into smart grids and with future technologies**:

   - Smart grid compatibility: The integration of solar-fed inverters with a smart grid environment can be easily achieved when it comes to fault detection. Enable advanced grid services, demand response, and dynamic interactions of the grid for improved system flexibility and resilience.
   - Future proofing: With technologies for fault detection in place, solar power systems would be assuredly adaptive and resilient to further changes and demands that may come in the energy landscape.

Thus, the implementation of detection of faults in multilevel inverters for solar-fed applications will ensure reliable, efficient, and safe power generation and grid integration. Maximum power harnessed, grid stability, cost reduction, and meeting the standards for regulation can all be assured with the high level of advancement in the detection of the fault technology for these appliances. Advancement in fault detection technologies should then continue to realize the promise of solar and enable sustainable energy solutions in making a greener planet.

CHAPTER 2

Fundamentals and Literature Review

This chapter is split into two main sections: the first covers the fundamental principles of PV systems and inverters, and the second provides a thorough review of existing methods and technologies used for fault detection in these systems.

2.1 Power electronic converters

Power electronic converters are essential components in numerous applications, such as electric vehicles, renewable energy systems, and power supplies. Converters can be broadly classified depending on the area of application, function, and topology. Major classifications include DC-DC converters, DC-AC inverters, AC-DC rectifiers, and AC-AC converters. A wide range of subtypes are included in these major classes for different voltage, current, and power applications.

DC-DC converters

DC-DC converters are devices for changing one level of direct current (DC) to another. They can also be classified as unidirectional or bidirectional, with each class available in both isolated version and non-isolated version.

- Unidirectional DC-DC Converters: There are two types: isolated converters—push-pull, full bridge, and flyback—and non-isolated converters which include Buck, Boost, and Buck-Boost converters.

- Bidirectional DC-DC Converters: These are able to accommodate current in both directions of flow. Single-stage converters, multi-level converters, and interleaved boost converters are included in this class.

DC-AC inverters

DC-AC inverters have the means to convert DC to alternating current (AC). They can be classified into two-level and multi-level inverters.

- **Two-Level Inverters:** These include single-stage and multi-stage converters, as well as conventional full-bridge inverters.
- **Multi-Level Inverters:** These are further divided into diode clamp, flying capacitor, cascaded H-bridge, hybrid, and dual inverters, which are used for high-power applications.

AC-DC rectifiers

AC-DC rectifiers have the ability to convert AC to DC and can be classified into two categories: single-phase and three-phase rectifiers. These are essential in power supplies and battery charging systems.

AC-AC converters

AC-AC converters modify the characteristics of AC power, including its voltage, current, frequency, or phase. They encompass cyclo converters and matrix converters, which are utilized in motor drives and variable frequency applications.

Figure 2.1 provides a comprehensive classification of power electronics converters. The top-level categories include DC-DC converters, DC-AC inverters, AC-DC rectifiers, and AC-AC converters. Each main category is further subdivided:

- **DC-DC converters:** These are split into unidirectional and bidirectional types, with further distinctions between isolated and non-isolated converters. Examples include Push-Pull, Flyback, and Multi-Phase Buck converters.
- **DC-AC inverters:** These are categorized into current source and voltage source inverters, with two-level and multi-level/phase subtypes. Notable examples include Full Bridge and Cascaded H-Bridge inverters.

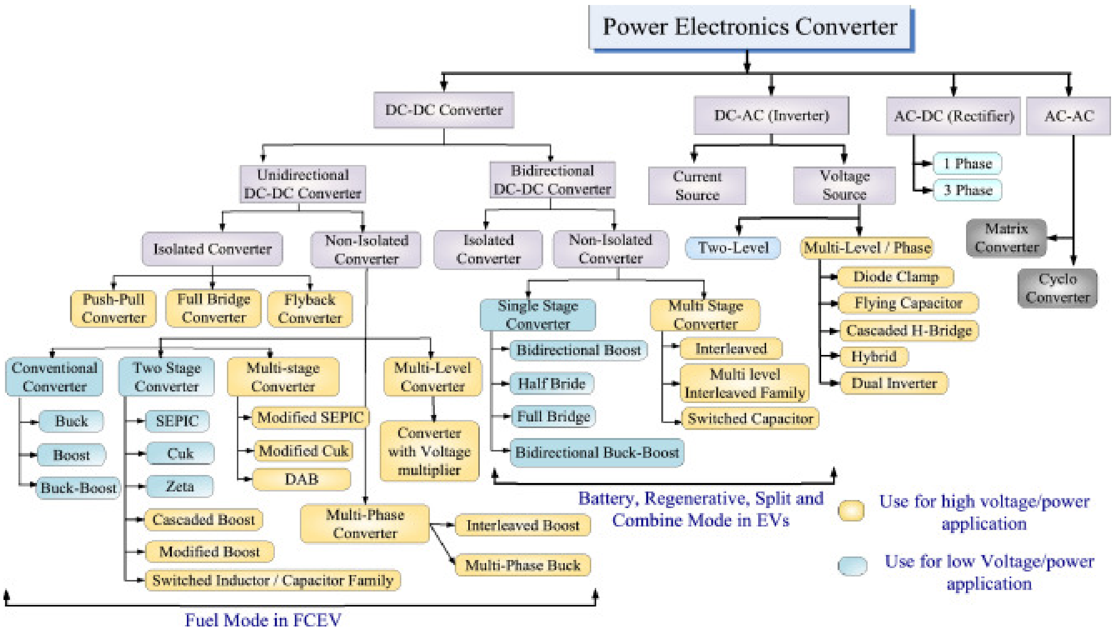

Figure 2.1: Classification of power electronics converters [20]

- **AC-DC rectifiers:** These are divided into single-phase and three-phase rectifiers, crucial for converting AC power to DC.
- **AC-AC converters:** This category includes cyclo converters and matrix converters, used to directly convert AC power from one form to another.

As shown in the image, a color code is made to show where these converters are used: yellow for high voltage/power applications and blue for low voltage/power applications. This is very helpful in that the classification given is very specific, helping users choose specifically what type of converter to use for a specific intended use, hence optimum performance and efficiency.

2.2 Inverters

An inverter, in regards to power electronics, is a crucial device that is able to convert direct current Direct Current (DC) into alternating current Alternating Current (AC) . It is very versatile in its uses; from household appliances to industrial machineries, machines, and renewable energy facilities. Inverters can be classified into several types on the basis of their design, operational principles, and applications. Here, we will focus on three primary types: single-level inverters, multilevel inverters, and specialized inverters.

2.2.1 Single level inverters

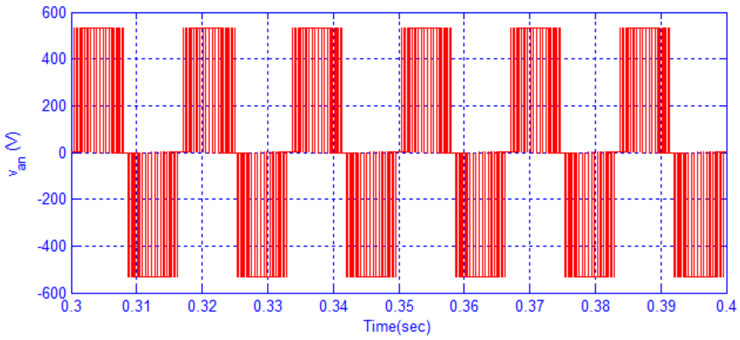

Figure 2.2: Two level inverter output [11]

Single-level inverters, also known as two-level inverters, are the simplest form of inverters. They convert DC to AC by switching the DC input voltage between positive and negative values, producing a square wave output as shown in figure 2.2.

Structure and operation

Single-level inverters typically use a single set of power switches (such as transistors or thyristors) to invert the DC voltage. These switches alternate the polarity of the input voltage, resulting in an AC output.

Advantages

- Simple in design, cost-effective, and easy to control.
- Suitable for applications where a basic AC output is sufficient, such as in small uninterruptible power supplies (UPS) and motor drives.

Limitations

The square wave output of single-level inverters has high harmonic content, leading to poor power quality and potential issues in sensitive equipment. Filtering techniques are often required to mitigate these harmonics.

2.3 Multilevel inverters

Multilevel inverters represent a significant advancement in inverter technology, offering improved power quality and efficiency. They generate multiple voltage levels from a set of DC sources, resulting in a stepped approximation of a sinusoidal waveform. The primary types of multilevel inverters include:

Neutral point clamped inverters

Neutral Point Clamped (NPC) inverters are important members of the multilevel inverter family, in addition to the diode-clamped multilevel inverters. They find use in applications ranging from medium- to high-power. The applications of these inverters are extended to the field of industrial motor drives, power supplies for renewable energy systems, grid-connected power supplies, and others where output waveform quality is of prime importance to bring down harmonic distortion and maintain overall efficiency. NPC inverters produce several levels of voltage by connecting the neutral point of the DC bus with diode clamps to the output phases as shown in 2.3.

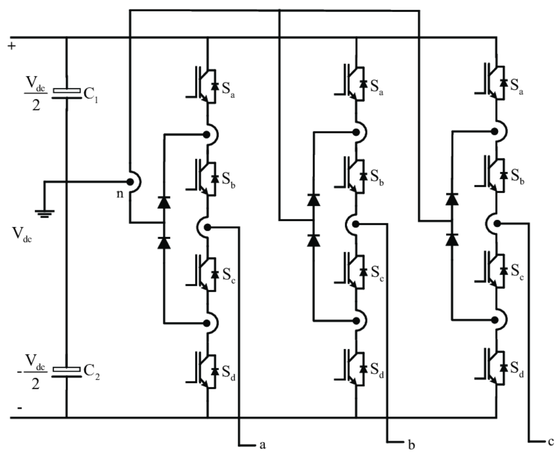

Figure 2.3: Three level NPC inverter [32]

As shown in figure 2.3, the basic three-level NPC inverter consists of the following:

- DC bus capacitors: These capacitors partition the DC bus voltage into two equal partitions hence creating a neutral point.
- Clamping diodes: These diodes clamp the center point of the DC bus capacitors to the output phases, thus permitting intermediate voltage levels.

- Switching devices: Typically, metal-oxide-semiconductor field-effect transistors (MOSFETs) and insulated gate bipolar transistors (IGBTs) are used to regulate the voltage levels applied to the load.

In the three-level NPC inverter, the output voltage has three possible values: zero, positive DC bus voltage or negative DC bus voltage. This comes from proper switching of the power devices and using the clamping diodes to limit the stress of the voltage on the switches.

Flying capacitor inverters

Flying Capacitor (FC) inverters or capacitor-clamped multilevel inverters are a type of multilevel inverter that utilizes capacitors as its primary elements to achieve numerous voltage levels. Particularly, these inverters are capable of generating high-quality output waveforms with low harmonic distortion, thus making them particularly suitable for medium to high power applications, such as industrial drives, renewable energy systems, and power grid interfaces. The configuration of an FC inverter comprises many capacitors and switches arranged in a way that they can produce a number of different voltage levels as illustrated in figure 2.4.

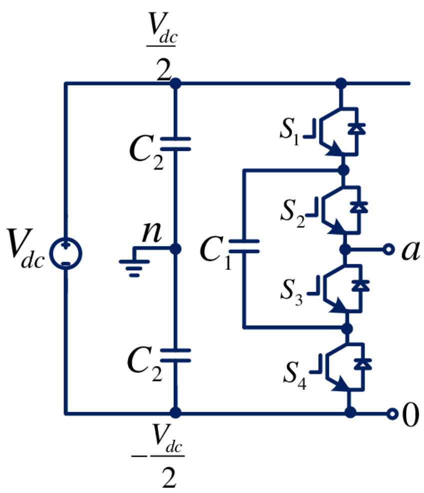

Figure 2.4: Flying capacitor inverter [2]

Some of the main elements of an FC inverter include:

- Switching devices: The common switching devices used are metal-oxide-semiconductor field-effect transistors (MOSFETs) or insulated gate bipolar transistors (IGBT). These devices are utilized to control the level of voltage present at the output.

- Flying capacitors: These capacitors are connected in series with the switching devices and are used to clamp the voltage to intermediate levels between the main DC bus voltages.
- DC bus capacitors: These capacitors store the main DC supply voltage for the inverter.

For an n-level FC inverter, the number of voltage levels, n, is decided by the number of flying capacitors and switching devices used. For instance, a five-level inverter will have four flying capacitors. The capacitors charge and discharge in a controlled manner, allowing the inverter to generate stepped output voltages that approximate a sinusoidal waveform.

Cascaded H-bridge Inverters

The CHB inverters are a type of multilevel inverter architecture that is quite suiting for medium to high power applications. These inverters find wide application in motor drives, renewable energy systems, and power grid interfaces due to their capability to produce high-quality output waveforms, scalability, and modular design. The CHB inverter is an assembly of several H-bridge cells connected in series. Each cell in the H-bridge can produce three different voltage levels: positive, zero, and negative. The total output voltage is the sum of voltages generated by each H-bridge cell. A single H bridge is shown in figure 2.5.

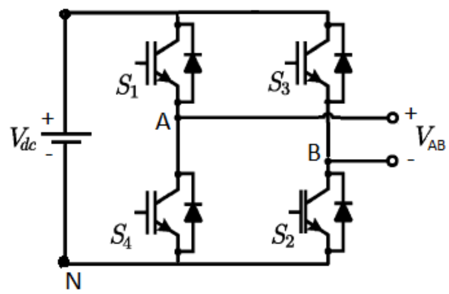

Figure 2.5: H-Bridge inverter [1]

Some important components of a CHB inverter are:

- H-Bridge cells: Each H-bridge cell is a full-bridge inverter comprising four switching devices, typically metal-oxide-semiconductor field-effect transistors (MOSFETs) or insulated gate bipolar transistors (IGBTs) , along with a DC power source.
- DC power sources: These can be separate DC sources, batteries, capacitors, or photovoltaic panels, depending on the application.

- Control system: The control system manages the switching of each H-bridge cell to synthesize the desired output waveform.

Advantages of multi level inverters

MLIs are designed to produce output voltage waveforms that closely approximate a sinusoidal shape by synthesizing multiple discrete voltage levels. Figure 2.6 shows the comparison of different levels of voltages. These levels are 2 levels, 3 levels and 5 levels.

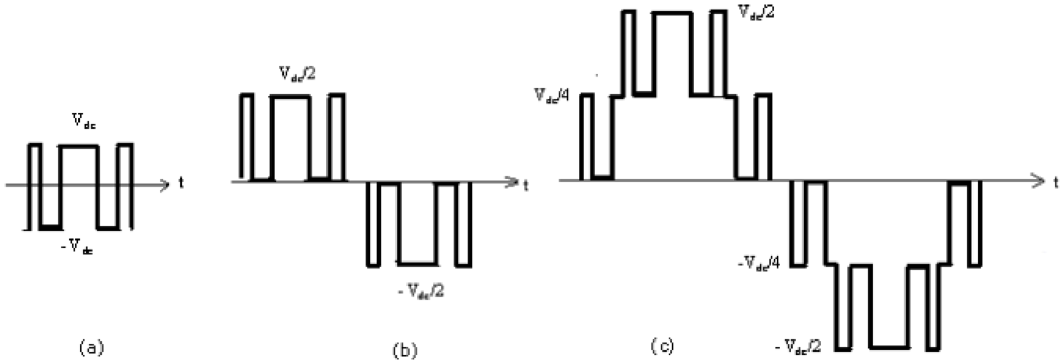

Figure 2.6: Comparison of output voltage waveforms [34]

The advantages of MLIs include:

- Improved output waveform: The stepped output waveform closely approximates a sinusoidal wave, resulting in the reduction of Total Harmonic Distortion (THD) and improving power quality.
- Higher efficiency: Lower switching losses and better utilization of the DC sources contribute to higher overall efficiency.
- Scalability: The modular design of multilevel inverters allows for easy scaling to higher power levels by adding more H-Bridge units or other modules..

Challenges of Multilevel Inverters

1. **Complex control:** Precise timing of the switching events is required for multilevel inverters, which makes their control strategies more complex since the output waveform has to be of the desired shape.

2. **More components:** Switches, diodes, and capacitors mean increasing the number of components, which in turn increases cost and complexity.

3. **Fault detection and management:** Reliable operation at this increased order of magnitude of components and potential fault points necessitates effective fault detection and management strategies.

2.4 Specialized inverters

1. **Grid tied inverters:** These inverters are integral to renewable energy systems, converting DC power from sources like solar panels and wind turbines into AC power that aligns with the grid. They frequently incorporate features such as Maximum Power Point Tracking (MPPT) to optimize energy harvest and anti-islanding protection to ensure safety and reliability.

2. **Stand-alone inverters:** Used in off-grid systems where the inverter provides AC power independently of the grid. This is the major part of their application, which is normally done in remote or backup power systems and often includes battery management features.

3. **Bidirectional inverters:** A bidirectional inverter can perform the task of converting DC to AC and vice versa. It is normally utilized for purposes like battery energy storage systems and charging stations of electric vehicles. The existence of bidirectional flow management lends compatibility between inverting operations to have a flexible solid-level energy management system.

Converters are the most diversified and indispensable elements in the domain of modern power electronics. There exist many different types of inverters, designed to cater to the different requirements of applications. Single-level inverters are simple and relatively inexpensive; multilevel inverters offer better power quality and efficiency; and specialized inverters are designed and optimized for specific applications. It is important to know the nature, merits, and problems of each class of inverter so that an appropriately suitable inverter can be chosen for a particular application.

2.5 Overview of H-bridge inverter

An H-Bridge multilevel inverter comprises several H-Bridge units, each of which has three levels of voltage: positive, zero, and negative. These modules are connected in a series format to obtain the staircase waveform, which approaches the ideal sine wave. This configuration results in a reduced level of THD for the output voltage and is hence related to significant generation of quality power. H-bridge topology finds an advantage in this regard as it can ease the control strategy used and lower the component count.

Working principle

The working principle of an H-Bridge multilevel inverter lies in the procedure followed in switching the states of the power semiconductor devices (IGBTs or MOSFETs) for each H-Bridge unit. Properly timed switching events allow the inverter to deliver a stepped output voltage waveform, which is near sinusoidal. This stepped waveform is created from the sum of the voltages generated by each of the H-Bridge units, offering better resolution for controlling the output voltage and frequency.

Applications in renewable energy systems

There is an ever rising demand to integrate renewable sources of energy with the electricity grid, and hence, for more effective power conversion systems. H-bridge multilevel inverters are applied in various applications of renewable energy, particularly in photovoltaic (PV) systems. Such inverters convert DC power developed from solar panels into an appropriate AC suitable for grid integration or local consumption. Their most basic utility within the PV system is that they have the capability of maintaining high efficiency while managing very high power levels. By distributing the voltage among many H-Bridge units, the multilevel approach lessens the strain on individual components. By doing so it achieves increased reliability of the inverter overall coupled with an ability to work more easily under conditions of differing loads. In addition to PV systems, H-Bridge multi-level inverters are used for wind energy conversion systems, battery storage systems, and electric vehicle charging stations. It is preferable due to its high performance and flexibility for many renewable energy applications.

Advantages

H-Bridge multilevel inverters have several advantages, making them in wider application. Some of the key benefits include:

1. **Improved output waveform quality:** The multilevel approach will lead to a staircase output

voltage waveform close to a sinusoidal wave, thereby reducing the THD and requiring high filtering to be decreased.

2. **Reduced switching losses:** Working with the H-Bridge topology at low switching frequencies attains lower switching losses and further increases the overall efficiency.

3. **Scalability and modularity:** The whole architecture of the H-Bridge makes it very modular to scale an inverter simply by placing more H-Bridge units in series for handling more power.

4. **Enhanced Reliability:** Chances of component failure will be significantly lowered when voltage stress is distributed to a great number of H-Bridge units. Hence this enhances reliability and longevity.

Challenges

1. **Complex control strategies:** Control of multiple H-Bridge units demands algorithms sophisticated enough to secure the exact timing of switching events to uphold the desired output voltage waveform. Development and realizing the control strategies might be difficult, and at times, computationally heavy.

2. **Increased component count:** The modular nature of H-Bridge multilevel inverters means more components than simpler inverter topologies are necessary. This may eventually lead to higher costs and space requirements.

3. **Fault detection and management:** More the number of components and design complexity, more an inverter design needs appropriate fault detection and management strategies. Reliable operation under fault conditions is a major goal for the practical success of H-Bridge multilevel inverter. Multilevel H-bridge topologies offer many advantages in terms of quality, effectiveness, and reliability of the output waveforms; hence, they have been popular for renewable energy systems. However, these features also increase the complexity and call for enhanced control and fault-detection mechanisms to reap maximum benefits from such inverters.

2.6 Solar energy

Overview of solar power generation

The generation of solar power harnesses energy from sunlight through PV cells, transforming it directly into electricity through the technology known as 'photovoltaics'. Such a process uses key components and steps as follow:

1. **Photovoltaic cells:** PV cells are semiconductor devices, mainly composed of silicon, absorbing photons from sunlight. In fact, this absorption excites electrons, thus leading to direct current (DC) electricity.

2. **Solar panels:** PV cells are connected in series and parallel connections to make a solar panel by which the output current and voltage can be heightened for use.

3. **Solar arrays:** Many solar panels combine to generate tremendous electricity suitable for applications within homes, offices, or even large uses by power utilities.

2.7 Overview of photovoltaic energy

Lately, there's been a growing interest in different sources of electrical energy because of the plentiful sunlight and their eco-friendly advantages. The most common use of this energy is in rural areas where no public electricity is available. Material research and technological advancement in semiconductors, used to build photovoltaic cells, have significantly come in as a boost in fast growth and development of this renewable energy. One of the key challenges of PV systems is extracting the maximum solar energy, as the efficiency of the installation drastically depends on sunlight and ambient temperature. The development of techniques for real-time maximum power extraction, such as the Maximum Power Point Tracking (MPPT) technique, has been done by this impact. At the same time, another solution would be to increase the presence in an electric network with a PV inverter having active harmonic filtering capability, given that non-linear loads are quite intensive. The key is to furnish an FAP-GPV topology in which solar energy extraction is maximized, together with the energy quality reaching the level required by international standards and norms.

A PV system utilizes solar panels for the conversion of solar energy into electrical energy with the help of several components, including PV panels, electrical connections, mechanical connections, regulation systems, and conversion systems. The significance of PV cells can be explained as a component made up of semiconductor materials like silicon. These semiconductors have been designed into cells that can be used effectively both in series and parallel[27]. To form an electric field in a PV cell, a semiconductor wafer (silicon) is used, consisting of a negative side and a positive side.

As shown in Figure 2.7 When light makes contact with a solar cell, electrons are emitted from

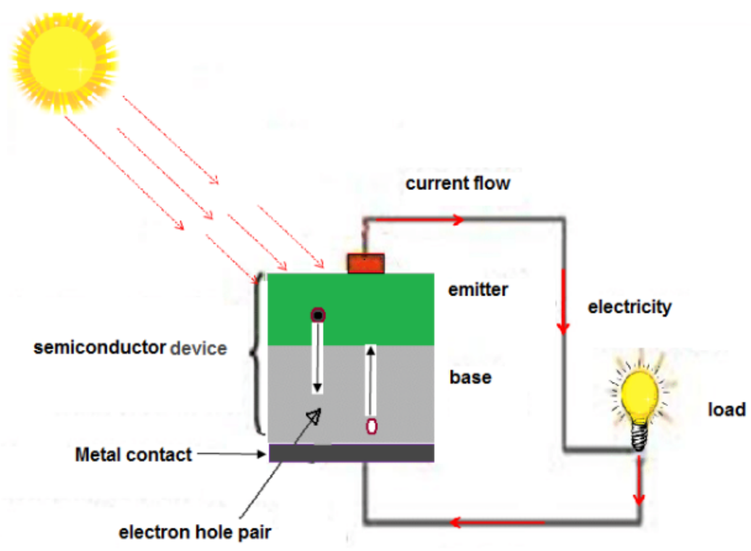

Figure 2.7: PV cell [15]

the atoms of the semiconductor material. These freed electrons can then be captured, generating an electric current at the output of the solar cell.

The use of solar energy through photovoltaic systems has observed a significant increase in recent years, driven by the growing global crisis awareness of environmental sustainability and the urgent need to reduce greenhouse gases. Solar PV technology is a key player in the transition to clean and sustainable energy sources. The sun panels that capture sunlight and transform it into DC electricity, constitutes the heart of the photovoltaic system. However, to fully exploit solar energy and integrate it with our current energy without any problem equipment, the efficiency of the conversion of DC to AC is required.

2.8 Safety and protection of photovoltaic panels

When designing a photovoltaic installation, it is essential to ensure the electrical protection of the system to extend its lifespan and prevent destructive failures related to the association of cells and their operation under shading conditions. A solar panel is composed of several interconnected cells. To prevent a damaged cell from affecting the holistic performance of the panel, a safety system is integrated using protection diodes. There are two types of diodes used for this purpose:

- Series diodes (Anti-return diodes): These are added to prevent reverse currents.

- Parallel diodes (Bypass diodes): These protect shaded cells by diverting the "normal" current, preventing it from passing through the "shadowed" cell and minimizing production loss.

These protective measures are crucial in maintaining the efficiency and reliability of photovoltaic panels, ensuring that the system continues to function effectively even when individual cells are compromised. A solar panel typically contains one to three bypass diodes, depending on the number of cells it has (on average, 36 cells for 3 bypass diodes).

Advantages of solar power

1. **Renewable:** Solar energy is an unlimited resource and can be the consistent substitute for conventional fossil fuel.

2. **Environment friendly:** Generation of solar power does not produce any greenhouse gas emissions in operation, reducing carbon footprint.

Challenges of solar power

- **Intermittency:** Solar power generation depends on the availability of sunlight, which fluctuates with weather conditions and the time of day.
- **Initial cost:** The upfront cost of solar panels and associated equipment can be high, although prices have been decreasing over time.

Role of DC-DC converters in PV systems

DC-DC converters are crucial components in solar power systems, serving to regulate and optimize the voltage output from solar panels. Their primary functions include:

Voltage regulation

The solar panels generate a variable direct current voltage based on sunlight intensity and temperature. The DC–DC converters control proper and stable voltage for the inverter and other components of the system.

Maximum power point tracking

Normally, MPPT is embedded within the DC-DC converter control algorithms and carries out the job of extracting as much power as possible from the solar panels. The electrical operating point of the modules or arrays is regulated so they always operate at maximum power.

Efficiency improvement

By optimizing voltage and current output, DC-DC converters enhance overall efficiency within a solar power system by converting and using more energy in the process.

Types of DC-DC converters

- **Buck converters:** It is a step-down converter that reduces the input voltage to a lower, regulated output voltage. This method is opted when the desired output voltage is lower than the input voltage.
- **Boost converters:** It is a step-up converter that increases the input voltage to a higher, regulated output voltage. This is opted when the desired output voltage is higher than the input voltage.
- **Buck-Boost converters:** These converters are versatile enough to provide either a higher or lower regulated output voltage in comparison to the input voltage.

Advantages of DC-DC converters

- **Improved system performance:** Stability in the output power of voltage and power extraction optimization are advantages that a DC-DC converter brings in a solar system..
- **Flexibility:** There are several available DC-DC converters available that can meet different voltage regulation needs and, therefore, highly flexible in use regarding different solar power applications.
- **Protection:** DC-DC converters can be designed with additional features such as overvoltage protection, overcurrent protection, and thermal management for the safeguarding of the components.

2.9 Integration of solar power with multilevel inverters

The integration of solar power with multilevel inverters involves several key steps to ensure efficient and reliable power conversion:

DC output from solar panels

The solar panels generate DC voltage whose level varies in accordance with sunlight intensity and environmental conditions.

Voltage regulation through DC-DC converters

The DC output from the solar panels is fed to the DC-DC converters wherein the voltage is adjusted and optimized using MPPT algorithms.

DC input to multilevel inverter

The multilevel inverter receives the regulated DC voltage from the DC-DC converters. It converts this DC voltage into the AC voltage that can be delivered at the end-use or fed into the grid.

Multilevel inverter operation

The multilevel inverter synthesizes the AC output by generating multiple voltage levels from the regulated DC input. This gives high-quality AC output with less harmonic distortion.

Benefits of integration

- Higher efficiency: Integrating optimally designed DC-DC converters along with multilevel inverters provides more efficiency in the overall solar power system.
- High quality power output: Multilevel inverters produce a high-quality AC waveform with lower THD, making them better compatible with grid standards and sensitive equipment.
- Scalability: The modularity of both DC-DC converters and multilevel inverters allows ease of scaling to fulfill increased power demand.

Modern power systems are therefore highly dependent on solar energy and DC-DC converters that provide a renewable and efficient source of electricity. In this regard, the addition of solar power to multilevel inverters is particularly advantageous in terms of power quality, efficiency, and scalability.

2.10 Faults in H-Bridge inverters

H-Bridge inverters, like all power electronic devices, can develop different types of faults. It is important to understand these faults, their origins, and consequences, to be able to put in place efficient strategies in detection and mitigation. This section mainly discusses the different types of faults that may occur in H-Bridge inverters, with a focus on open-switch faults, their impacts on system performance, and fault detection methods.

Types of faults in H-bridge inverters

1. **Open switch faults:**
   - Description: This is a type of fault that takes place if one of the semiconductor switches (IGBTs, MOSFETs, and so forth) employed within the H-Bridge fails to conduct current—it becomes an open circuit.
   - Causes: These faults are consequential from component aging, thermal stress, manufacturing defects, or control signal failures.
   - Consequences: Open switch faults can cause unbalanced output voltage levels, a rise in harmonic distortion, reduced efficiency, and possibly damage other parts due to abnormal current flows.
2. **Short circuit faults:**
   - Description: Fault due to short-circuit occurs when a switch fails in the permanently closed condition and thereby creates a direct short across the power supply or load.
   - Causes: Such faults may be caused by overvoltage conditions, insulation failures, or catastrophic breakdown of the component.
   - Consequences: Short-circuit faults can lead to high overcurrent states, which have the potential to destroy the inverter, power supply, and load. Instant actions with protection are needed so that the failure is not catastrophic.

3. **Gate driver faults:**

   - Description: The anomalies in control signals driving switches can lead to wrong switching actions.
   - Causes: These defects may be due to some trouble in the control circuit, signal interferences, or power supply to the gate drivers.
   - Consequences: Improper switching may result in suboptimal inverter performance with increased losses or even cause stress and failure in components.

4. **Thermal faults:**

   - Description: Components may get heated too much and this heating may lead to thermal runaway or even degradation, hence causing thermal faults.
   - Causes: Overloading, lack of cooling, or high ambient temperature.
   - Consequences: Continuous exposure to high temperature shortens the lifespan of components, causes efficiency to drop, and raises the probability of other kinds of faults.

Consequences of open switch faults

Open switch faults are one of the commonest and most critical types of faults that occur in H-Bridge inverters. Some of the more specific consequences are:

1. **Unbalanced output voltage levels:** An open switch results in the disruption of the intended switching sequence, which causes asymmetry in the output voltage waveform. This can consequently lower power quality and enhance harmonic distortion.

2. **Increased harmonic distortion:** As a result of poor switching action, deviations from the ideal output waveform are noticed, which in turn increases the THD. Increased THD would result in inefficiencies and associated difficulties in supplied loads.

3. **Reduced efficiency:** Open circuit faults prevent the inverter from being used at its efficient point of operation. The resulting inefficiency tends to increase energy losses and lower system performance.

4. **Potential damage to components:** The unusual current paths developed due to this fault of an open switch can exert some sort of stress on the other components of the inverter that might lead to more faults, and finally failure of these components.

Consequences of short switch faults

The short switch faults in 5-level CHB inverters can have severe implications for the performance and reliability of the entire system. These faults will cause an unwanted continuous conduction of the switch or will create a low resistance path and generate a few critical problems.

1. **Excessive current flow:** The fault related to short switches can lead to a high current peak up to more than two times the maximum peak set value. The overrated current, if present, might induce overtemperature on some components, leading to permanent damage of the inverter switches, power semiconductors, and other related hardware. It may also cause protective devices to trip, leading to interruptions in the supply of power and possible downtime.

2. **Increased power losses:** Abnormal current flow because of short switch faults can lead to substantial losses in power in the system. It lowers the overall energy conversion efficiency of the solar energy system and gives additional heat that further stresses and degrades the system components.

3. **Component damage and reduced lifespan:** With the continuous operation under a short switch fault condition, the wear and tear rate of components is significantly increased, reducing their lifetime. Critical components, such as capacitors, inductors, and power semiconductors, may suffer increased thermal and electrical stress, resulting in premature failure that requires expensive repairs or replacement.

4. **System instability and potential safety hazards:** A slight fault in the switch may easily cause the normal operation of the inverter to be disturbed, thus leading to system instability. This instability can manifest as voltage and current fluctuations, which may adversely affect other connected systems or equipment. In severe cases, these faults can pose safety hazards, such as electrical fires or electric shocks, particularly if the fault leads to insulation breakdown or exposes live parts.

Addressing short switch faults promptly and effectively is crucial for maintaining the integrity and safety of the solar energy system and ensuring reliable power delivery.

2.11 Existing methods for fault detection

Fault detection is an important factor in controlling the adverse effects of the faults on H-bridge inverters. Quite a number of techniques have been developed, among them are:

Voltage and current monitoring:

- **Description:**Continuous monitoring of voltage and current waveforms is done. These help to identify any anomalies that may point to faults.
- **Advantages:** It is quite simple in implementation, and it can be done real-time.
- **Limitations:** May not always find the exact position or exact type of fault without additional analysis.

Thermal imaging:

- **Description:** Thermal cameras or sensors detect abnormal temperature rises in inverter components.
- **Advantages:** Non-invasive, hence provides visual confirmation of overheating components.
- **Limitations:** Detects only thermal faults and needs frequent monitoring and maintenance.

Signal processing techniques:

- **Definition:** Advanced signal processing algorithms analyze the inverter's electrical signals to detect characteristic fault signatures.
- **Advantages:** Can detect and diagnose a wide range of faults with high accuracy.
- **Limitations:** Needs sophisticated hardware and computational resources.

Model based approaches:

- **Description:** These use mathematical models of the inverter for the comparison of expected performance with actual measurements.

- **Advantages:** They can provide deep insights into the causes and locations of faults.
- **Limitations:** The accuracy of the models is very important; and accurate models may be cumbersome to develop.

Deep learning techniques:

- **Description:** In this approach, machine learning models, especially deep learning, are used to learn from historical fault data in such a way that they recognize and classify faults in real time.
- **Advantages:** High accuracy, ability to deal with complex patterns, potential for real-time implementation.
- **Disadvantages:** Very high demand for training data and computation power to train and run the models.

These recent advances, particularly in the domain of fault detection techniques using deep learning, bring new hope for increasing the reliability and efficiency of H-Bridge inverters in different applications.

2.12 Literature review

The research on detection faults in CHBMLIs has continued, from the viewpoint of the application of model-based strategies and advanced ML and AI techniques. The basic idea, key methodologies, and pursued approaches of researchers in the field of fault detection in CHBMLIs, including the use of model-based methodologies, machine learning, deep learning techniques, are presented herein.

The advancement in renewable energy technologies has significantly increased the reliance on solar power systems, particularly in the integration of sophisticated inverter architectures like the Cascaded H-Bridge 5 level Inverters. The robustness and efficiency of these systems are paramount, necessitating advanced fault detection mechanisms to ensure continuous and reliable operation. Over the past few decades, various methods and models have been proposed to address the challenges of fault detection in multi-level inverters. The broader picture of these methods is shown in figure 2.8 . This section reviews the existing literature on traditional and contemporary fault detection techniques, its trend in evolution, machine learning and deep learning models, and how these innovations improve reliability and performance in solar-fed inverter systems. This section identifies strengths and limitations of prior research, presenting a broad view of the present state-of-the-art concerning fault detection methodologies, laying the ground for this work.

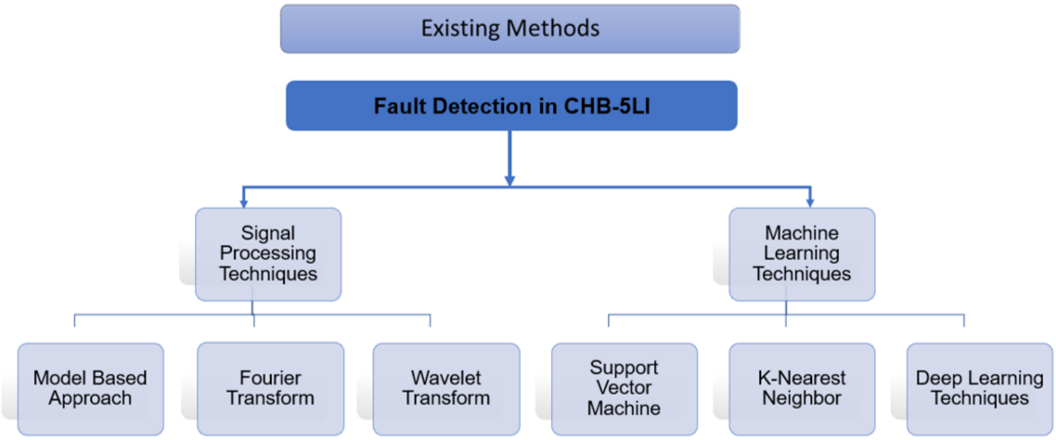

Figure 2.8: Existing methods for fault detection

The paper [22] proposed novel fault-tolerant scheme that enhances the reliability of CHB inverters, which are pivotal for generating high-quality AC outputs. In the event that a power switch fails, the proposed approach is to bypass the failed H-Bridge cell with the existing backup cell in place of the functionally lost one while restoring balanced line-to-line voltages from the CHB inverter. The system continues operating at maximum possible output voltage, using the remaining healthy cells fully operational with only limited operational losses to maintain reduced fault sensitivity of the proposed system. The authors in [13] illustrate a robust method to regain the operational performance of CHB inverters. The method is SVM-based and incorporated in an auxiliary unit to detect faults and recover operation; this system can bypass the faulty cell dynamically and, in this way, maintain the inverter's performance.

Model-based fault detection methods rely on accurately obtained mathematical models of cascaded H-bridge inverters. Such models react to deviations in the system behavior when open-switch faults are established. These methods include parameter estimation methods as well as observer based methods. Observer-based implementation techniques use state observers to estimate system states and compare them with actual measurements. If a significant discrepancy is observed, a fault is indicated.Whereas, in the parameter estimation method, parameters of the inverter model such as resistance and inductance are estimated and changes are monitored. A significant deviation from the nominal values indicates a fault. The authors in [18] have proposed the use of signal processing techniques where PWM asymmetries, reference signals, and resultant output voltages are analyzed to detect open transistor faults. Also, there are specific significant mean values for each faulty transistor that have been introduced due to the existence of the fault.

In another example, to detect and localize the fault, researchers have used Fuzzy Inference Systems (FIS) [30] and Model Predictive Control (MPC) [8]. The predictions given by the MPC controllers were compared with the actual measurements, and faulty switches were detected. However, these methodologies may run into difficulties in correctly capturing dynamic complexities and non-linearities of real systems, resulting in possible inaccuracies within fault detection, especially for multiple open switches.

Machine Learning (ML) and Artificial Intelligence (AI) tools and techniques provide alternative methodologies for fault detection in CHBMLIs through the use of historical data for learning the patterns associated with normal and faulty operation. In [3], the authors investigated the fault diagnosis of CHMLIs with ML algorithms mainly based on classification algorithms, where the k-NN and SVM algorithms were proposed. PPCA was implemented for feature extraction, and it was shown that the fault diagnosing speed was quicker by using SVM, while the accuracy increases, especially for CHMLIs with an open switch fault.

In [31] a 15-level inverter is examined for fault diagnosis.The fault diagnostic method proposed has the following architecture: a fully connected feedforward neural network layer, referred to as the multi layer perceptron, which identifies and then classifies whether a condition is normal or faulty in CHBMLIs. In[29], Shen et al. have implemented a unique convolution neural network (CNN) based diagnostic method for open switch fault diagnosis for neutral point clamped inverter, which features a dual input channel. Through this implementation, midpoint voltages, along with three-phase currents of the NPC inverter, serve as signals for the purpose of extracting fault information[24]. In [9], features are extracted via wavelet decomposition from single switch fault output and ANN to detect failure from open switch in a five level cascaded inverter. The wavelet decomposition process involves breaking down the signal into different frequency components at varying resolutions. By decomposing the signal into twelve levels, the researchers aim to extract detailed information about the signal's frequency content and identify specific patterns associated with open switch failures in the inverter system. Among the plethora of mother wavelets, the "dB10" wavelet is utilized, which belongs to the family of orthogonal wavelets, specifically the Daubechies wavelets.

In the context of PV systems, fault detection methodologies have also been investigated extensively. ML-based approaches, including Gaussian Process Regression and ANN techniques, have been employed for diagnosing various faults such as mismatch, partial shading, and short circuit faults [10] [25]. ANN architectures are mainly useful for fault detection using inputs such as solar irradiance, cell temperature, and PV current-voltage characteristics [10] [17]. Hybrid deep learning techniques have also been proposed for fault identification based on Electroluminescence (EL) imaging [36]. ANFIS and Clarke transformed assisted ANNs are used for open-circuit fault diagnosis and fault localization in switches (IGBTs) of three-phase inverters[6][21].

Research evidenced in this section clearly highlights diverse methodologies and approaches that have been employed for fault detection in CHBMLIs and PV systems. Whereas model-based strategies underpin efforts in fault detection, ML and AI techniques provide alternative promising avenues of research for addressing complex system dynamics in the improvement of detection accuracy. Researchers using historical data and advanced learning algorithms aim to develop renewable energy systems that are ever more reliable, performant, and safe, for global adoption of clean energy technologies.

CHAPTER 3

System Modelling

This chapter is intended to address the main focus of our research, which is to integrate a photovoltaic source into the inverter's DC bus (dc-link). This combination, also known as a PV inverter, offers several significant benefits, including the ability to supply free active power to the electrical grid alongside the active filtering option characteristic of Voltage Source Inverters (VSI). In this way, the active compensator is now capable of performing multiple functions: ensuring reactive power compensation, eliminating current-type harmonics, and ultimately supplying a certain amount of active power to the distribution network.

3.1 Mathematical modelling of photovoltaic system

This section addresses the mathematical modeling of Photovoltaic system which we integrated with CHBMLIs for our data source. Figure 3.1 illustrates the equivalent circuit of a PV cell, which consists of an ideal current source in parallel with a diode. The cell is exposed to real-world conditions of irradiance and temperature T.

In this model, the current source represents the photocurrent generated by the cell, which is directly proportional to the sunlight (irradiance) hitting the cell. The diode models the p-n junction of the cell, where the behavior of the diode is affected by the temperature of the environment. These factors influence the overall performance and efficiency of the PV cell, making it essential to consider both irradiance and temperature in the system's design and operation. Understanding this model is crucial for optimizing the power output and integrating the PV system effectively into broader electrical networks.

A single-diode solar cell can be shown by an equivalent electrical circuit as shown in figure 3.1

where I_{ph} represents the photogenerated of the connected PV module and I_{d0} is the average current of the diode. R_s represents the series resistance in the cell, which includes the resistance of the cell material, contacts, and interconnections, R_{sh}represents the parallel resistance, modeling the leakage paths across the cell, mainly due to defects and impurities.

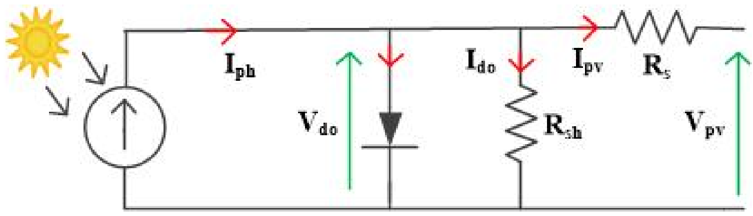

Figure 3.1: Equivalent electrical model of a photovoltaic Cell

A PV cell can be modeled using the equation that defines the static behavior of the PN junction of a conventional diode. Thus, the output current produced by a solar cell I_{pv} and the output voltage V_{pv} can be expressed as follows:

$$I_{\text{pv}} = I_{\text{ph}} - I_{\text{d0}} \left[\exp\left(\frac{qV_{\text{do}}}{nkT} \right) - 1 \right] - \frac{V_{\text{pv}} + R_{\text{s}} \cdot I_{\text{pv}}}{R_{\text{sh}}} \tag{3.1.1}$$

$$V_{\text{pv}} = V_{\text{do}} - R_s \cdot I_{\text{pv}} \tag{3.1.2}$$

These equations capture the relationship between the current and voltage of a PV cell, taking into account the effects of temperature and the intrinsic properties of the diode. It is fundamental for predicting the performance and optimizing the design of PV systems.

3.2 Connection of photovoltaic cells

Depending on the requirements and systems used, photovoltaic cells can be connected in series and/or parallel configurations. This association of cells results in a photovoltaic generator (GPV).

- Series connection: Boosts the voltage while keeping the current constant.
- Parallel connection: Boosts the current while keeping the voltage constant.

Combining multiple cells forms a module, and the association of several modules constructs a panel as shown in figure 3.2. A photovoltaic field is created by connecting multiple panels in series and/or parallel configurations.

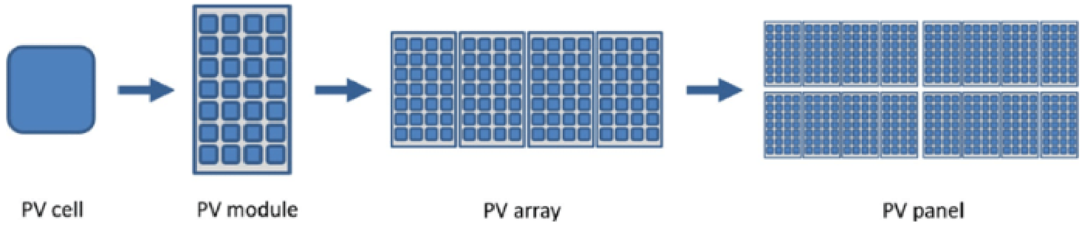

Figure 3.2: PV cell, pannel, module and array [16]

This modular approach allows for flexibility in designing PV systems to meet specific power requirements and optimize performance according to the available space and environmental conditions. From an energy efficiency standpoint, industrially, the following efficiencies can be achieved for different types of silicon-based cells:

- Monocrystalline silicon cells: 13% to 14%
- Polycrystalline silicon cells: 11% to 12%
- Amorphous thin film cells: 7% to 8%

These efficiencies reflect the current technological capabilities and the material properties of each type of cell. Monocrystalline cells offer the highest efficiency due to their high purity and uniform crystal structure, while polycrystalline cells, being less pure, offer slightly lower efficiency. Amorphous thin-film cells, though the least efficient, are cost-effective and flexible, making them suitable for various applications.

3.3 Current-Voltage characteristics with variable irradiance and temperature

Figure 3.3 illustrates the I-V (current-voltage) and P-V (power-voltage) characteristics of a solar cell, where P_m represents the maximum power point,I_{sc} denotes the short-circuit current, and V_{oc} indicates the open-circuit voltage. It can be inferred from the figure that for one specific point of operation, Maximum Power Point (MPP), the PV cell provides maximum power.

An I-V curve is a curve that plots the current-voltage relationship at various levels of irradiance and temperature. A P-V curve shows how the output power varies in relation to voltage. The maximum power point (MPP) refers to the point of maximum current multiplied by voltage in

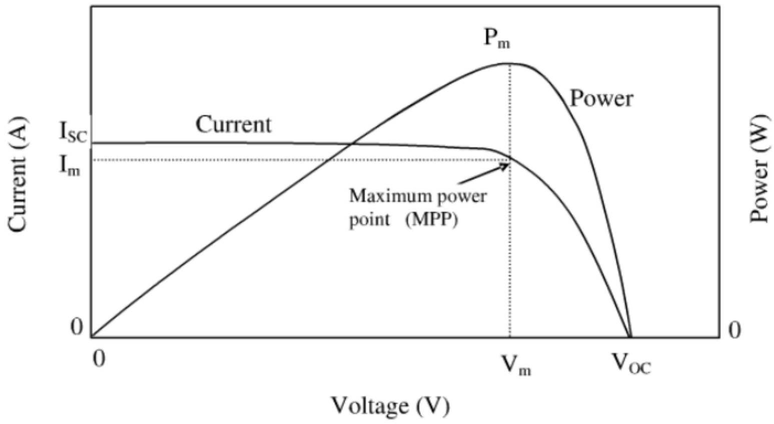

Figure 3.3: I-V P-V characteristics of solar panel [23]

the product of the two terms, I * V. Working at this point is of paramount importance to get optimum energy from a PV system. MPP represents the point on the I-V curve where optimal power corresponds. It can translate to the operating point where the best irradiation and temperature conditions are. It is necessary to operate at the MPP if a PV system is to be very efficient. Power output is maximum when this particular point of operation of the PV cell is obtained, taking all available sunlight and favorable temperature conditions into account. That makes MPPT a very important part of PV system design so that the system keeps working at or close to peak performance in any environmental condition.

Influence of irradiance

As previously mentioned, a photovoltaic cell is highly sensitive to changes in sunlight irradiation. Based on the I-V characteristics, the current is significantly influenced by changes in sunlight, while the voltage V remains approximately constant. Consequently, strong irradiation of 1000 W/m² generates an optimal current for the cell. Other parameters can also impact the panel's efficiency, such as geometric size and the angle of solar incidence. Maximizing irradiance on the PV cells ensures they produce the highest possible current, which is critical for achieving maximum power output. Therefore, proper placement and orientation of solar panels, considering these factors, are essential for optimizing the overall performance of a PV system.

Influence of temperature

However, when ambient temperature changes, the voltage V can vary while the current remains relatively unchanged. Figure 3.4 illustrates the characteristic curves under a range of variable temperatures from 0 to 75°C.

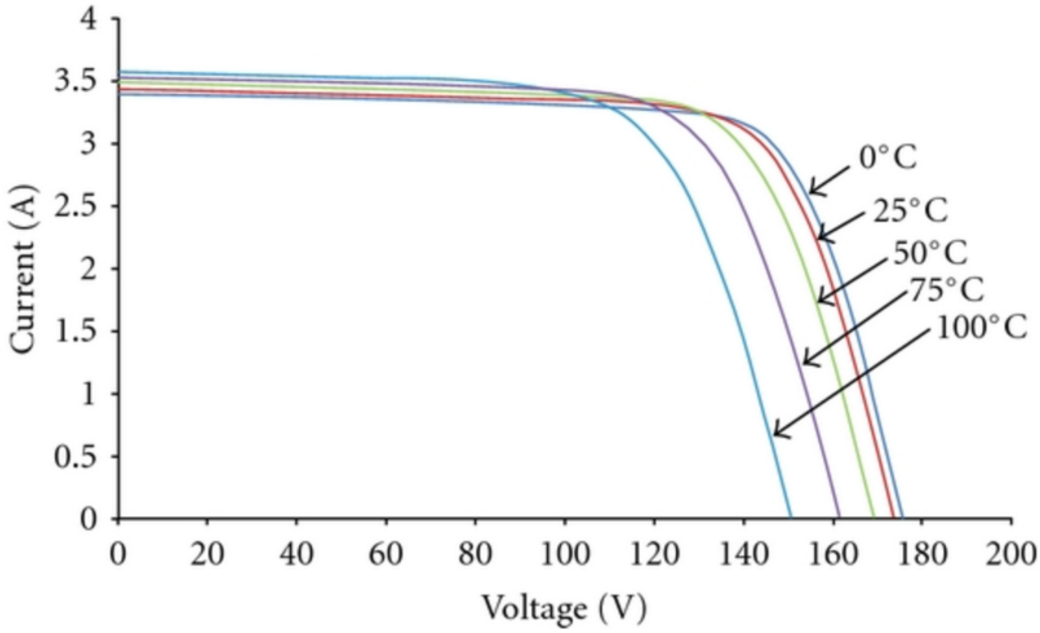

Figure 3.4: I-V characteristics of solar panel under different temperatures [35]

Temperature has a substantial impact on the performance of photovoltaic cells. As temperature increases, the open-circuit voltage Voc decreases, which affects the overall voltage output of the cell. This phenomenon is due to the intrinsic properties of semiconductor materials used in the cells. While the current is less affected by temperature variations compared to voltage, overall power output can still be affected as temperature changes alter the balance between voltage and current at the MPP.

Optimizing the temperature conditions around PV panels, such as through cooling mechanisms or proper ventilation, can help mitigate these effects and increase the efficiency and longevity of solar energy systems.

Maximum power point tracking techniques

The performance of PV cells depends on their output sensitivity to changes in irradiance. Because solar irradiance and temperature vary, it is important to trace the most available power of PV cells through effective control of an ordinary boost converter using the MPPT method. Very fundamentally, this MPPT extracts the maximum power from the PV panels by applying different control algorithms. These algorithms have their basis inn Perturb and Observe (P&O), Incremental Conductance, and other intelligent MPPT techniques related to fuzzy logic, ANN, or adaptive methods like ANFIS [5].

MPPT algorithms adjust the operating point of the PV system continuously to ensure it operates at or near the MPP, despite fluctuations in environmental conditions. This optimization maximizes the efficiency of the PV system, enhancing energy yield and overall performance over its operational lifespan.

3.4 DC-DC conversion stage

To consistently harness the maximum available power PV generator (GPV) and transfer it to the load, a DC-DC conversion stage must be employed. A boost converter (step-up converter) is an electrical device capable of directly connecting a voltage input source (generator) to a current output source (load). This stage serves as an interface between the two elements, ensuring efficient power transfer through control action, typically employing MPPT.

A boost converter functions as a voltage step-down device when the power switch (often a MOSFET) is placed in series with the load. It operates as a voltage step-up device when the switch is placed in parallel with the load. In many applications, the use of a boost converter is essential to maximize the output voltage of a photovoltaic system. In most cases, the DC-DC converter is controlled using MPPT techniques to maintain the highest possible efficiency (typically above 90%). The efficiency of the converter is primarily influenced by components such as the MOSFET transistor, smoothing inductors, and capacitors used for energy storage.

The circuit of a boost converter primarily consists of inductors, capacitors, a diode, and a controllable switch. These devices dissipate ideally no power at all, so the efficiency of the static converters is very high. Notice that the appropriate operation of these static converters depends on the appropriate selection of passive components such as the inductor for current smoothing and the output capacitor. These components will then assure efficient performance and proper operation that will guarantee stability in photovoltaic systems with the DC-DC converters.

3.5 Perturb and Observe algorithm

The most popularly identified MPPT techniques are the Perturb and Observe (P&O) algorithms. The operation principle is built upon perturbing the system, incrementing or decrementing the reference voltage Vref, or acting directly on the duty cycle, and observing the effects in the output power of the panel. The following is a detailed process for the operation of the P&O algorithm:

- Perturbation: The operating point is perturbed by increasing or decreasing V_{ref} or by adjusting the converter duty cycle.
- Power comparison: It compares current output power $P(k)$ with past output power, $P(k-1)$.
- Decision making: If $P(k)-P(k-1)>0$, it indicates that the power increased with the perturbation direction. Therefore, it continues perturbing in the same direction in the next iteration. If $P(k)-P(k-1)\leq 0$, it reverses the perturbation direction in the next iteration.

Figure 3.5 illustrates the flowchart of the P&O technique, depicting the sequential steps involved in adjusting and optimizing the operating point of the PV system to locate the maximum power point.

The Perturb and Observe (P&O) algorithm is straightforward to implement and effective in many PV applications. However, it may experience oscillations around the maximum power point, especially under rapidly varying irradiance conditions.

3.6 PV integration with power converter

The block diagram for PV system is shown in 3.6. A 5 level cascaded H bridge inverter (CHI) is used as power converter for the conversion of DC energy into AC energy, where the eight switches combined by (S_1- S_4) upper bridge and (S_5- S_8) lower bridge are integrated in the main circuit of the inverter as shown in 3.7 . Two bridges are used to generate 5 level voltage. This is because each cell can provide a maximum of three levels of voltage, thus limiting the

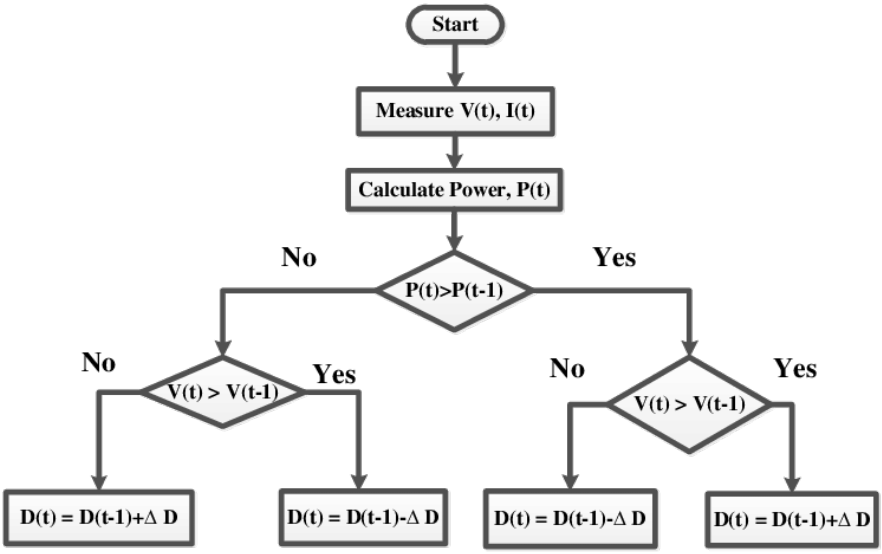

Figure 3.5: P&O MPPT algorithm [33]

maximum voltage level of each output phase at 2n + 1, where n signifies the number of the cells per phase[28]. The Vdc is voltage source from PV acting as input to these bridges.

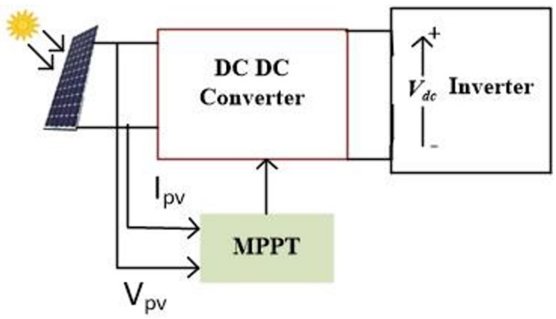

Figure 3.6: Block diagram for PV system

In this study, we employed multicarrier Sinusoidal Pulse Width Modulation (SPWM) to modulate a Cascaded H-Bridge Multilevel Inverter (CHB-MLI). To generate the PWM signals for the 5-level Cascaded H-Bridge inverter, we utilized a carrier-based PWM approach with a sinusoidal carrier waveform. This technique involves comparing a sinusoidal reference signal against several high-frequency triangular carrier signals. The outcome of this comparison dictates the switching states of the inverter's power devices, resulting in the desired multi-level output voltage waveform. The carrier-based PWM technique is crucial for achieving precise control of the inverter, enhancing efficiency, and reducing harmonic distortion.

This scheme compares multiple triangular carriers with a reference sinusoidal signal in order to generate the gate pulses. Table 3.1 shows the switching states for the 5-level H-bridge inverter.

"0" denotes that the matching switch is in the OFF state, and "1" indicates that the related switch is in the ON state [4]. Four carrier waves are compared with sine wave to generate PWM signals for the switching devices. The switching devices used in the inverter are MOSEFETs.

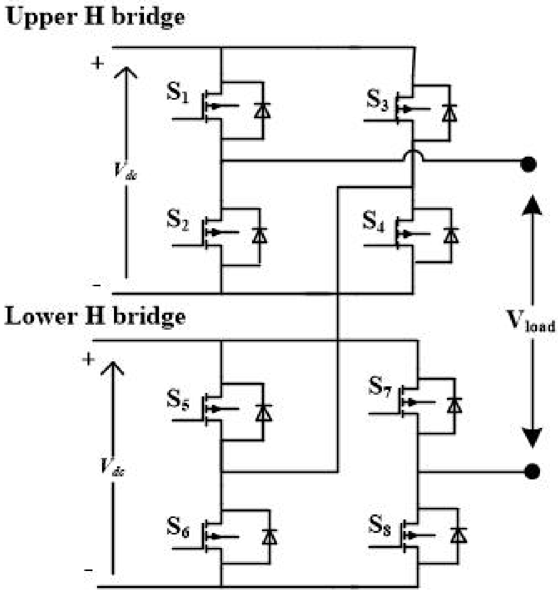

Figure 3.7: 5 Level H-bridge multi-level inverter

Sr #	Voltage	Switching State (S_1 to S_8)							
		S_1	S_2	S_3	S_4	S_5	S_6	S_7	S_8
01	2V	1	0	0	1	1	0	0	1
02	V	1	0	0	1	0	1	0	1
03	V	0	1	0	1	1	0	0	1
04	0	0	1	0	1	0	1	0	1
05	-V	0	1	1	0	0	1	0	1
06	-V	0	1	0	1	0	1	1	0
07	2V	0	1	1	0	0	1	1	0

Table 3.1: Switching states for 5-level H-bridge inverter

Figure 3.8 shows the integration of PV with CHBMLIs. In this model we have amended the weather conditions such as temperature and incident solar irradiance. The rays from the sun is converted to DC by PV array. The cells are connected in a combination of both series and parallel. The solar panel specifications used is given in table 3.2.

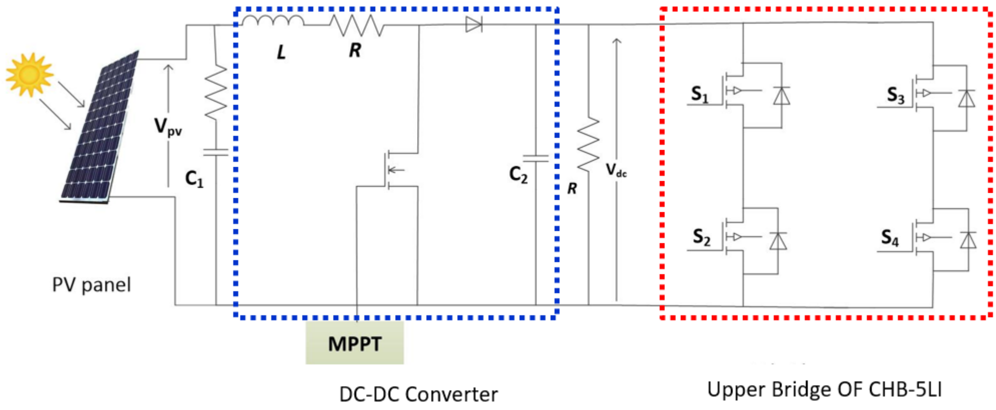

Figure 3.8: Schematic diagram for integration of PV with upper bridge of inverter

Parameters	**Value**
Max Power	214.89 W
Cells per module	60
Open circuit voltage	34.8 V
Short circuit current	8.3 A
Maximum voltage point	29 V
Maximum current point	7.41 A
Irradiance	1000 W/m^2
Temperature	[45 25] °C
Diode saturation current	6.08 e-11 A
Ideality factor	0.883

Table 3.2: Solar panel specifications

Power output from the solar panels is maximized MPPT. Solar panels have a non-linear voltage-current (V-I) characteristic, and there exists a point on this curve known as the MPP, where the power (product of current and voltage) is at its peak as decribed earlier. We implemented the Perturb and Observe (P&O) method. This algorithm operates by periodically adjusting either the voltage or current and observing the resulting change in power output. By employing the P&O algorithm, the operating point of our PV system is dynamically adjusted, ensuring it consistently delivers maximum power, thereby enhancing overall system efficiency.

Figure 3.9, 3.10 and 3.11 illustrate alternative power source configurations aimed at managing the variability of solar energy inputs and enhancing system reliability in the context of 5-level

CHB inverter where in figure 3.9 both bridges are supported by solar. In figure 3.10, the upper bridge of the inverter is supported by DC voltage source, while the lower bridge is supplied by a solar energy . This hybrid configuration leverages the stability of DC power to complement the intermittent nature of solar energy, thereby improving overall system reliability.

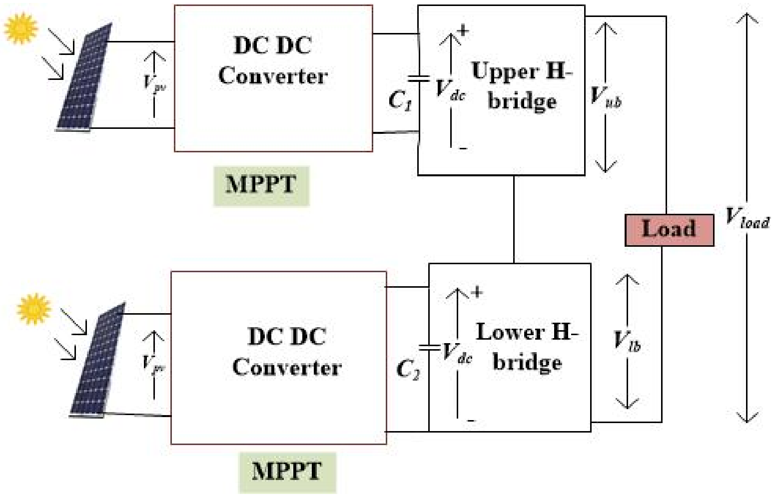

Figure 3.9: Case 1 PV integration with 5-level CHB inverter

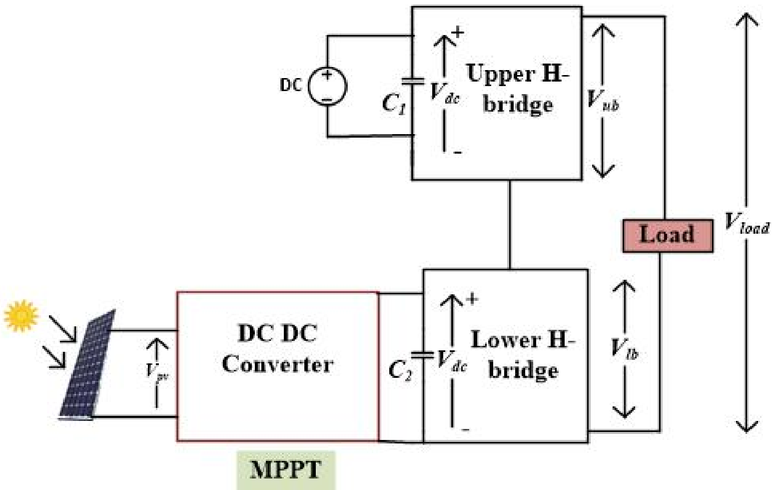

Figure 3.10: Case 2 PV integration with 5-level CHB inverter

Conversely, figure 3.11 depicts a configuration where the upper bridge is supported by a solar energy, while the lower bridge operates on DC voltage source . This arrangement offers another approach to balance power variability, ensuring continuous operation and minimizing disruptions in energy generation. By integrating these configurations with advanced fault detection systems tailored for 5-level CHB Inverter, our research aims to address critical challenges in renewable energy systems. The goal is to enhance the robustness, reliability, and real-time per-

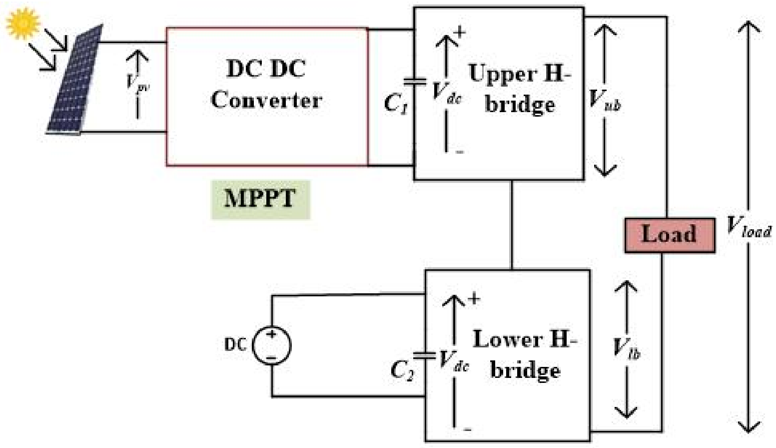

Figure 3.11: Case 3: PV integration with 5-level CHB inverter

formance of fault detection mechanisms, ultimately contributing to the seamless integration of solar energy into mainstream power grids and advancing sustainable energy solutions.

3.7 Conclusion

This chapter has provided a comprehensive understanding to the modeling of PV systems. It began by introducing the essential components of PV systems, including detailed diagrams of PV cells that illustrate their structure and operation. The discussion then shifted to various MPPT techniques, which are crucial for optimizing the energy output of PV systems by continually adjusting to the most efficient operating points. Furthermore, the chapter explored the integration of PV systems with a five-level H-bridge inverter. This integration is key to enhancing the performance of solar energy systems, as it allows for improved harmonic performance and reduced voltage stress compared to traditional inverters. By modeling these interactions, the chapter provided insight into how advanced inverter technologies can be employed to achieve more efficient and reliable solar power systems.

CHAPTER 4

Proposed Methodology

This chapter presents the methodology adopted in this research, designed to approach comprehensively the solution of the problem of fault detection in solar-fed, five-level CHB inverter. The chapter is arranged such that it brings out the processes involved in data collection, preprocessing, and the implementation of the deep-learning technique.

4.1 Block diagram

The proposed methodology for detection of fault and its classification in a solar fed CHBMLI involves several sequential stages as shown in Figure 4.1. Integrating a DC-DC converter to optimize the solar panel output, followed by a single-phase 5-level CHB inverter for efficient DC to AC conversion. Data collection then captures voltages across bridges, which further go through preprocessing. The data is then fed into a deep learning model. Various models and algorithms are explored, including their architecture, training processes, and performance evaluation and evaluated using different performance metrics. Based on those performance metrics, optimal model is chosen for the detection and classification of fault.

4.2 Data collection

In this research, we have focused primarily on the single short switch and upto two open switch faults, which correlates to rise in secondary failures as well in converter components. This can result in high repair costs [7].The output voltage along with upper and lower bridge voltage is collected for varying modulation indexes i.e. 0.55 to 1. The modulation index (m) is a

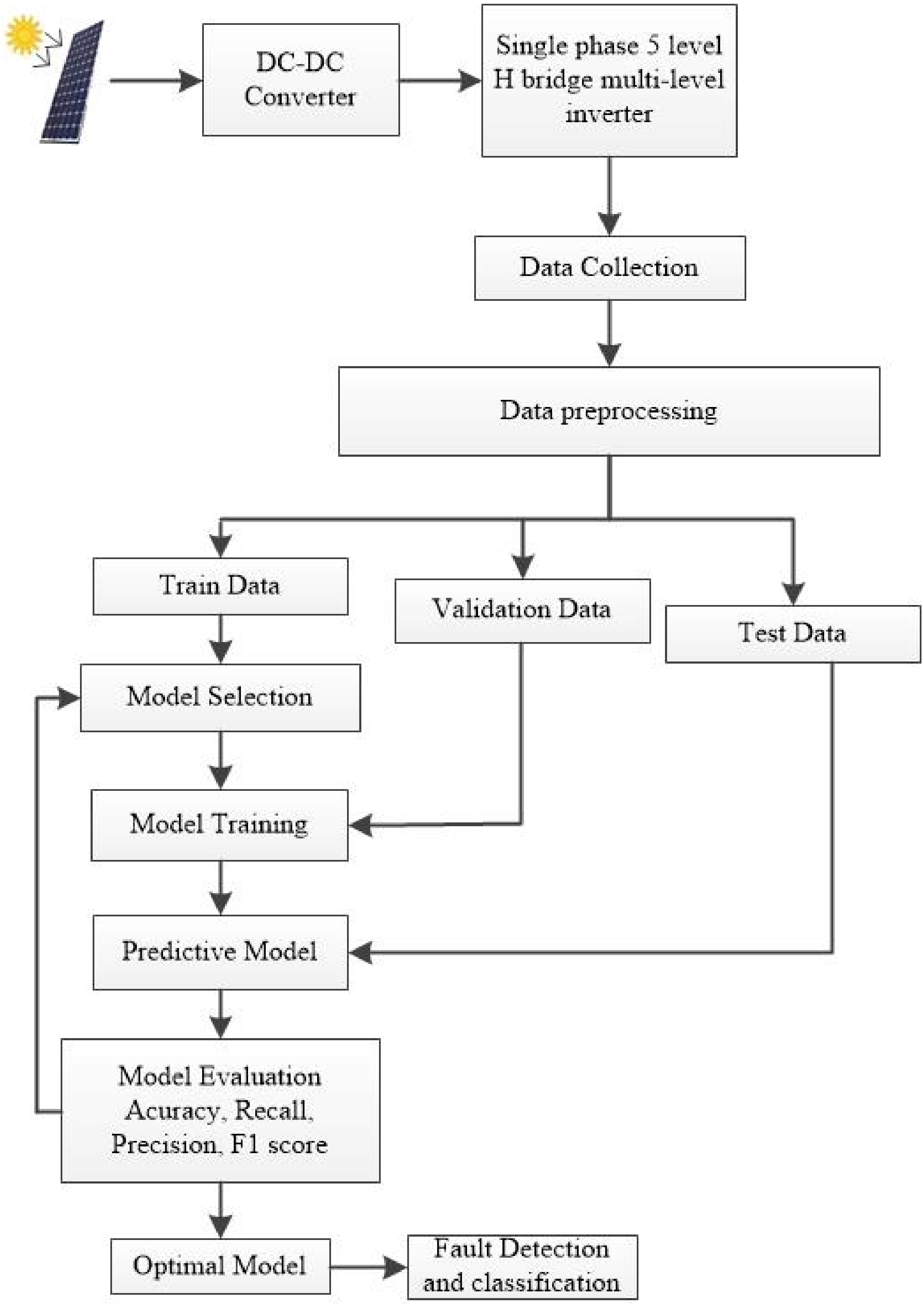

Figure 4.1: Block diagram

dimensionless quantity used in modulation applications. It is the ratio of the amplitude of the modulating signal's to the amplitude of the carrier signal. Mathematically, modulation index is defined in equation 4.2.1.

$$m = \frac{V_{\text{peak}}}{V_{\text{carrier}}} \tag{4.2.1}$$

In equation 4.2.1 m represents the index of modulation, V_{peak} is peak amplitude that the modulating signal can reach and V_{carrier} represents the peak amplitude that the carrier signal can reach.

The data comprises 49 unique fault cases, i.e. single and double open switch faults, single short switch faults, dc-dc converter switch fault, alongside an additional case representing fault absence, totalling 49 cases. Each case consists of three voltages as features pertinent to the operational parameters of the inverter.

No fault cases

Figure 4.2, 4.3 and 4.4 shows wave-forms for no switch fault in all 3 cases. It can be seen in 4.3 and 4.4 that it takes longer time to stabilize the output voltage because of mismatch in input voltage sources in each bridge.

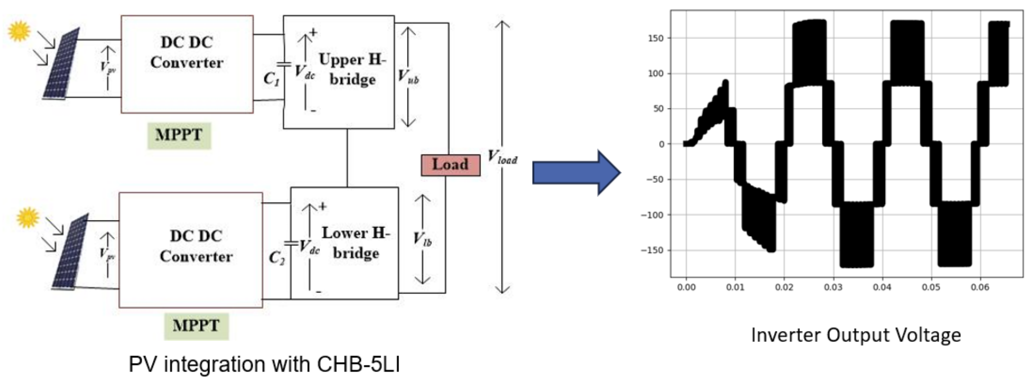

Figure 4.2: No switch fault case 1

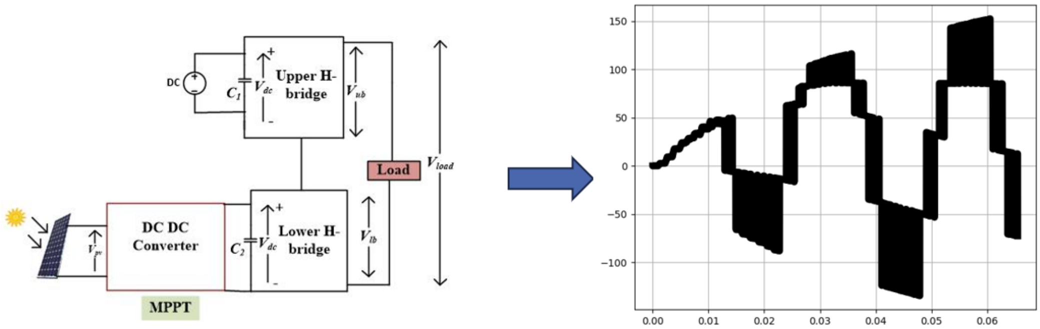

Figure 4.3: No switch fault case 2

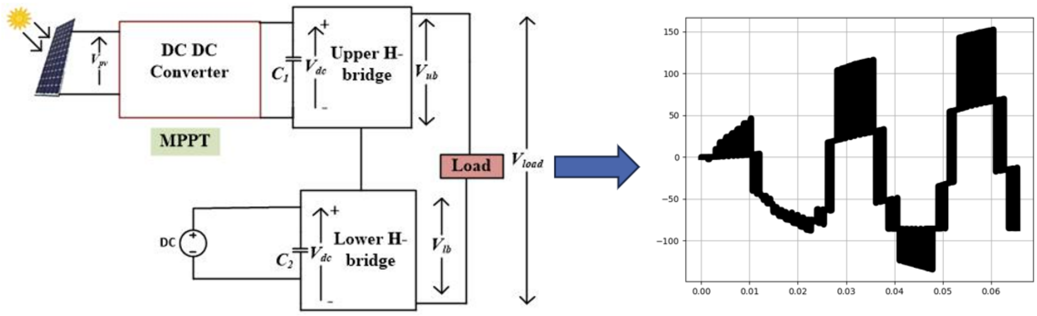

Figure 4.4: No switch fault case 3

Open circuit switch faults

Figure 4.5 shows wave-forms for single open switch fault cases. As shown in figure, there are 8 switches in CHB5LI so that makes 8 cases for single open switch faults. The waves differ in voltage levels. 28 classes belong to double switch faults in CHB5LI, and remaining belong to DC-DC inverter switch fault. Some of those faults are shown in figure 4.6.

H bridge short switch faults

Similarly figure 4.7 shows wave-forms for single short switch fault case where switch 8th is shorted. There are total 8 switches in H bridge that makes 8 classes for single H bridge short switches.

DC-DC converter switch faults

Scenario 1: Open Switch in the Lower DC-DC Converter

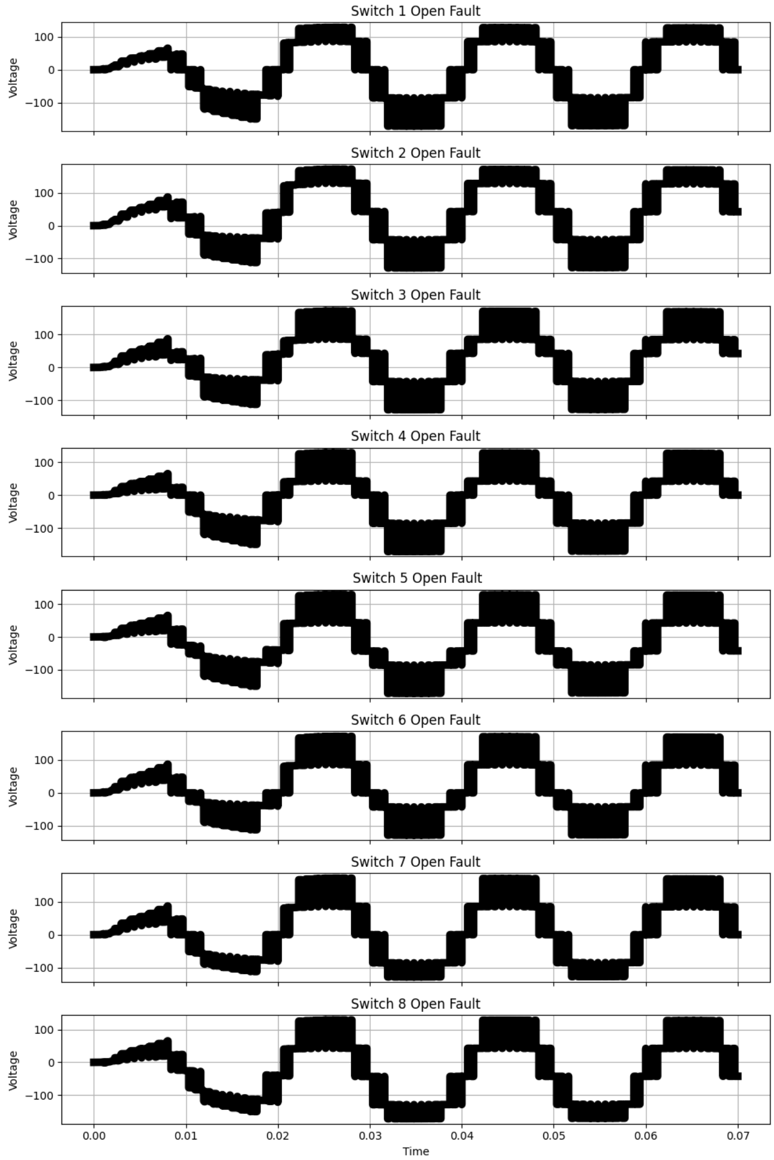

Figure 4.5: Single open switch fault types

When the lower DC-DC converter switch is open (no duty cycle signal):

- Inductor Behavior: The inductor attempts to maintain current flow, which results in a large voltage spike due to Lenz's Law.
- Voltage Overshoot: This high voltage spike can be significant, causing a temporary overshoot in the output voltage.
- Effect on Inverter Input: The upper bridge receives a normal regulated voltage, while the lower bridge experiences a high-voltage spike.
- Inverter Output: The high-voltage spike from the lower bridge creates an imbalance, caus-

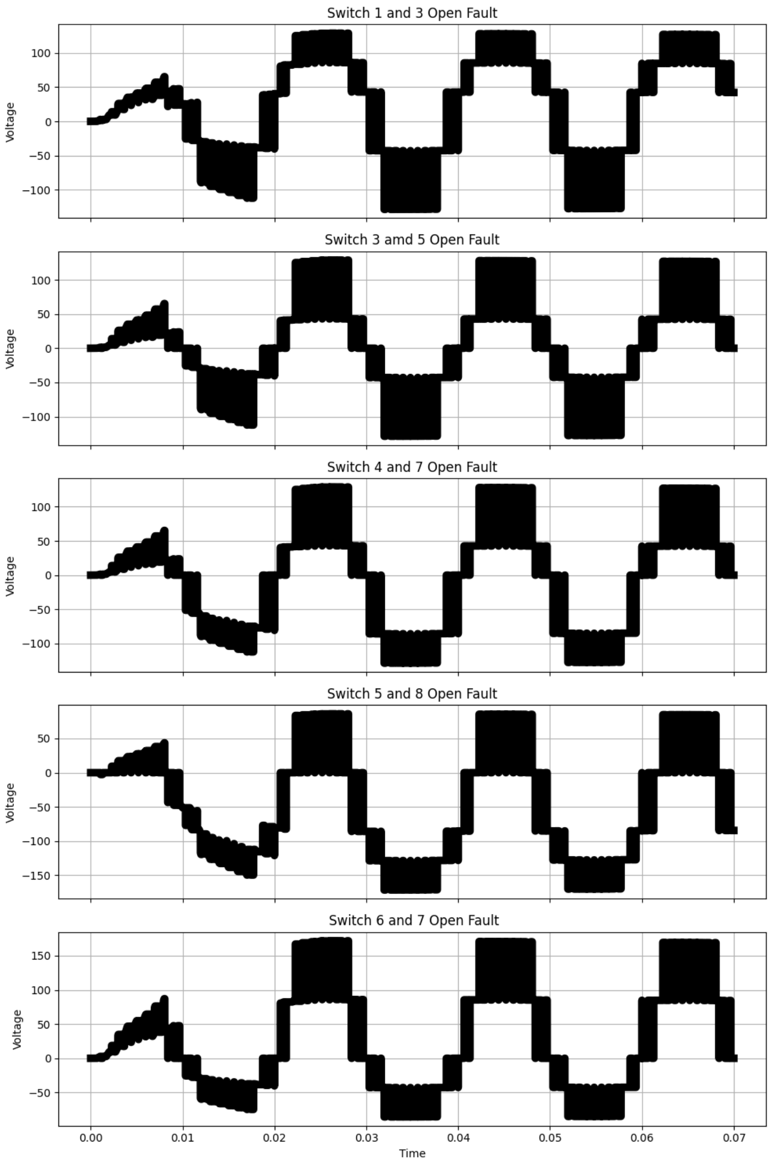

Figure 4.6: Double open switches fault types

ing the inverter output voltage to swing drastically between -1000V to 1000V. The control system of the inverter becomes unstable due to the sudden and large voltage changes, leading to longer stabilization time.

Figure 4.8 shows wave-forms for single open switch fault case where case 2 dc- dc switch is open.

Scenario 2: Shorted Switch in the Lower DC-DC Converter

When the lower DC-DC converter switch is shorted:

- Inductor Behavior: The inductor is directly connected to the input voltage, causing a

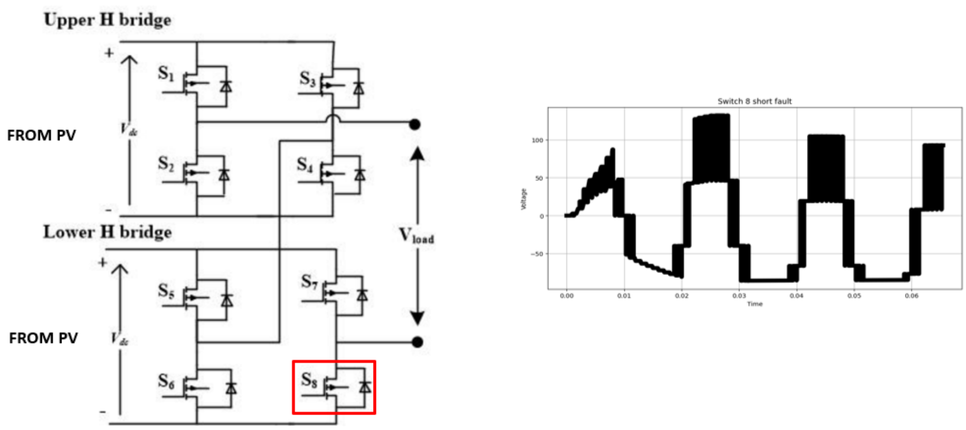

Figure 4.7: Single switch short fault types

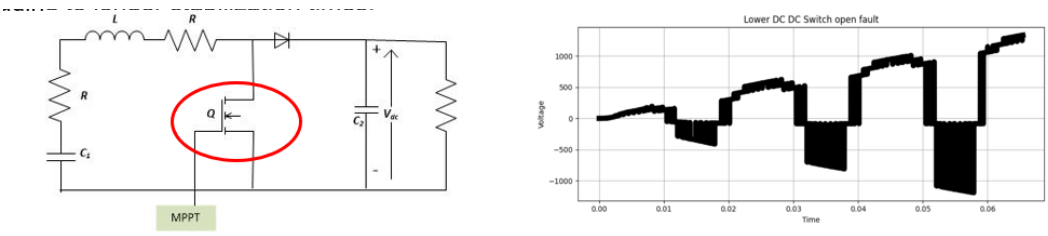

Figure 4.8: Single DC-DC converter switch open fault

current ramp-up through the inductor.

- Voltage Drop Across Switch: There is a small voltage drop across the shorted switch due to its internal resistance (Rds(on)) and other resistive elements.

- Effect on Inverter Input: The lower bridge receives a lower-than-expected DC voltage because the shorted switch bypasses the regulation mechanism, leading to a direct, unregulated (and likely lower) voltage.

- Inverter Output: The lower contribution from the lower bridge results in a reduced voltage swing in the inverter output, observed as -80V to 80V. The reduced input voltage from the lower bridge leads to an overall lower output voltage from the inverter, but with a more balanced and stable output compared to the open switch scenario.

Figure 4.9 shows wave-forms for single short switch fault case where dc- dc switch is open.

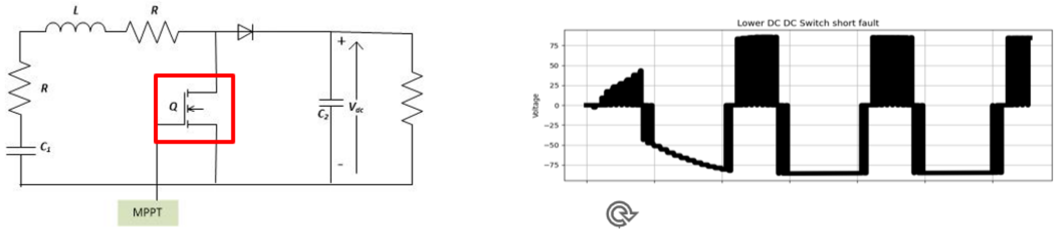

Figure 4.9: Single DC-DC converter switch short fault

4.2.1 White gaussian noise

In the context of fault detection in solar-fed 5-level CHB inverters, introducing White Gaussian Noise (WGN) into voltage signals plays a critical role in simulating real-world conditions and enhancing the robustness of fault detection algorithms. Incorporating WGN into voltage signals during the data collection and preprocessing stages is essential for several reasons:

1. **Realistic simulation**: The addition of noise opens further possibilities for realistic simulation of the actual operating conditions of the PV fed CHBMLIs. This simply states that models for fault detection are trained and assessed in a more realistic environment, implying that this enhances better practical applicability. By introducing noise, a model will learn to discriminate between real faults and anomalies induced by noise.

2. **Robustness and reliability**: This will make the fault detection system more robust and reliable, thus ensuring that it is not prone to false positives and negatives.

3. **Performance evaluation**: Actually, testing developed algorithms for fault detection under noisy conditions is a more stringent measure of performance. This would help one know how robustly the models would retain accuracy and consistency in any demanding situation.

WGN is defined statistically: it has a constant spectral density, meaning it is white over all frequencies, and its amplitude distribution follows the Gaussian or normal distribution. This makes it an ideal candidate for the simulation of random noise in voltage signals.

- Spectral density: The power spectral density (PSD) of WGN remains flat over the range of all frequencies. This property is necessary for the voltage signals since the noise affects each of them equally, therefore leading to an overall test environment for the fault detection algorithms.

- Gaussian distribution:The amplitude of WGN is Gaussian and given in terms of a mean (μ) and standard deviation (σ). For all practical purposes, the value of μ is zero, therefore making the noise center around zero and the parameter σ controls the spread, or intensity of the noise.

Mathematically, WGN $n(t)$ added to a voltage signal $v(t)$ is shown as:

$$y(t) = v(t) + n(t) \tag{4.2.2}$$

In equation 4.2.2 $y(t)$ depicts the noisy signal, $v(t)$ is the original voltage signal, and $n(t)$ is the WGN.

The noise $n(t)$ is characterized by its mean μ and variance σ^2:

$$n(t) \sim \mathcal{N}(\mu, \sigma^2) \tag{4.2.3}$$

In practice, the noise is described by its power, which is usually measured in units of decibels (dB). The SNR, known as the ratio between signal and noise, can be calculated in decibels as shown in equation 4.2.4.

$$\text{SNR}_{\text{dB}} = 10\log_{10}\left(\frac{P_{\text{signal}}}{P_{\text{noise}}}\right) \tag{4.2.4}$$

where P_{signal} is the original voltage signal power, and P_{noise} is the power of the noise.

To bring the noise level under control, set the power in the noise P_{noise} as follows:

$$P_{\text{noise}} = \frac{P_{\text{signal}}}{10^{\text{SNR}_{\text{dB}}/10}} \tag{4.2.5}$$

The standard deviation, σ, of the noise can be obtained from the power in the noise by taking the square root, as shown in equation 4.2.6.

$$\sigma = \sqrt{P_{\text{noise}}} \tag{4.2.6}$$

In the implementation phase, WGN is generated and added to the voltage signals utilized for the training and then testing the deep learning models.

This research aims to develop fault detection models that are not only accurate but also resilient to the noise and variability inherent in real-world renewable energy systems. We introduce WGN at various SNR levels, specifically -20 decibels, -10 decibels, 10 decibels, and 20 decibels, to assess the models' performance under different noise conditions.This approach ensures that the models are robust and reliable, ultimately contributing to the improved performance and safety of solar-fed 5-level CHB inverters. Figure 4.10 shows no fault ideal case i.e. with no noise, and a no fault case after incorporating WGN of -20db.

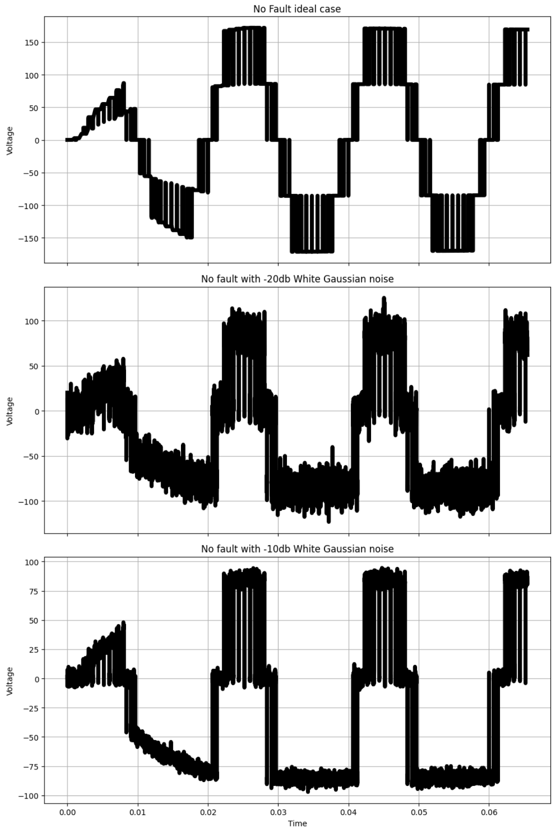

Figure 4.10: White gaussian noise

4.3 Data Preprocessing

The preprocessing technique for voltage signals from an CHB5LI involves two steps: first, applying a Moving Average Filter (MAF) having a window size of 10, and second, performing Wavelet Denoising. This two-step process smooths the data and removes noise while preserving significant signal features that are levels as shown in 4.11.

Moving average filter

The Moving Average Filter smooths the time-series data $x(t)$ by averaging the data points within a specified window size $N = 10$. This reduces short term noise and fluctuations, making the underlying trend more apparent. The smoothed signal $y(t)$ is given by:

$$y(t) = \frac{1}{10} \sum_{i=0}^{9} x(t-i) \tag{4.3.1}$$

Denoise wavelet

Wavelet denoising goes one step further to remove noise from the smoothed signal $y(t)$. The signal has a decomposition to its frequency components done through wavelet transformation, followed by thresholding of wavelet coefficients to remove noise and then reconstructed.

1. **Decomposition**: The Haar wavelet decomposes the smoothed signal, $y(t)$, into wavelet coefficients. The coefficients $c_{j,k}$ are computed as:

$$c_{j,k} = \langle y(t), \psi_{j,k}(t) \rangle = \int_{-\infty}^{\infty} y(t) \psi_{j,k}^{*}(t), dt \tag{4.3.2}$$

2. **Threshold Calculation**: In soft thresholding, threshold is derived by Stein's Unbiased Risk Estimate (SURE) based on the median absolute deviation of the coefficients. The threshold λ is:

$$\lambda = \sigma \sqrt{2 \ln(N)} \tag{4.3.3}$$

   where $\sigma = \frac{1}{0.6745} \cdot \text{MAD}$ and the length of the signal $y(t)$ is given by N.

3. **Soft Thresholding**: Soft thresholding is applied to the detail coefficients $c_{j,k}$ using the calculated threshold:

$$\hat{c}_{j,k} = \text{sign}(c_{j,k}) \cdot \max(|c_{j,k}| - \lambda, 0) \tag{4.3.4}$$

4. **Signal Reconstruction**: Reconstruct a denoised signal $\hat{y}(t)$ using thresholded wavelet coefficients.

$$\hat{y}(t) = \sum_{j=0}^{J} \sum_{k} \hat{c}_{j,k} \psi_{j,k}(t) \tag{4.3.5}$$

   where J is the number of decomposition levels.

Wavelet denoising using the Haar wavelet offers an effective method for preprocessing voltage signals contaminated with noise. By decomposing the signal into wavelet coefficients, applying soft thresholding, and reconstructing the denoised signal, unwanted noise is effectively removed while preserving important signal features. This preprocessing step significantly enhances the quality and reliability of voltage signal analysis and interpretation. Figure 4.11 shows the noisy signal, denoised signal obtained through MAF and wavelet denoising, and the residual signal highlighting the removed noise components.

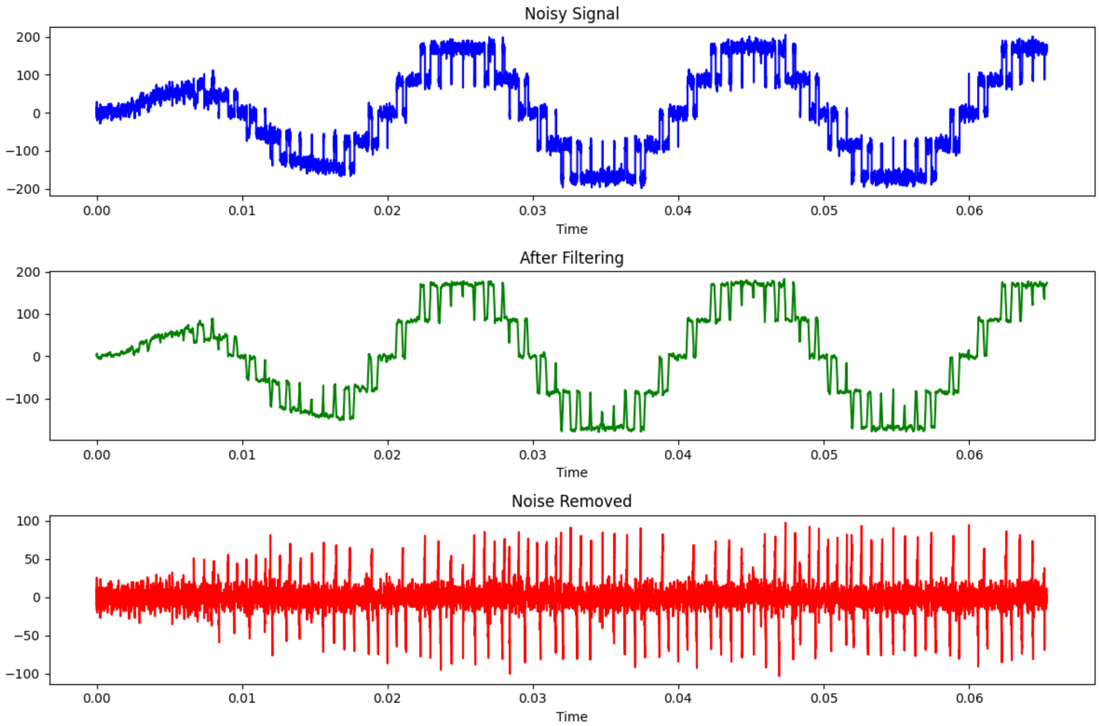

Figure 4.11: Signal denoising

Encoding

Label encoder is used to transform the classes into numerical values ranging from 0 to 48 (number of categories - 1). Label encoding assigns a unique integer to each category in a categorical feature. This encoding assumes an ordinal relationship between categories [26].

4.4 Deep learning techniques

We implemented several state-of-the-art deep learning models including Fully Convolutional Network (FCN), Long Short Term Memory (LSTM), ResNet, and a hybrid amalgamation of the CNN and LSTM architecture, CNN-LSTM model for time series classification to accurately identify and localize switches fault. Here, we discuss each model's architecture, technical aspects, and the results obtained.

4.4.1 Convolutional neural network

Convolutional Neural Network (CNN) is a specialized deep learning model applied to grid-like structured data and include images and time-series data processing. In fact, since CNNs are very effective in pattern recognition, there have been many successful applications from image classification and object detection up to the recent application in power electronics for fault detection. The 1D CNN model developed applies convolutional filters across the input sequence to capture the local patterns and dependencies in sequential data. The part of the architecture of CNN receives the input data, which goes under processing by applying convolution with a kernel to extract features in the form of feature maps. These feature maps capture relevant patterns or trends that vary over time within the signal, suggesting dynamic behaviors or transitions between different states and amplitude variations that are changes in the magnitude or intensity of the signal over time, reflecting fluctuations in the underlying phenomenon being measured. The 1D CNN's core operation is a convolution that uses a sliding window to apply multiple learnable filters (or kernels) on the input sequence, where each filter slides over an input sequence using a sliding-window approach and computes a feature map highlighting local patterns and features.

The FCN model is constructed using input layer, Convolutional Layers, Batch normalization, activation function, global average pooling and dense layer as shown in 4.12 [14].

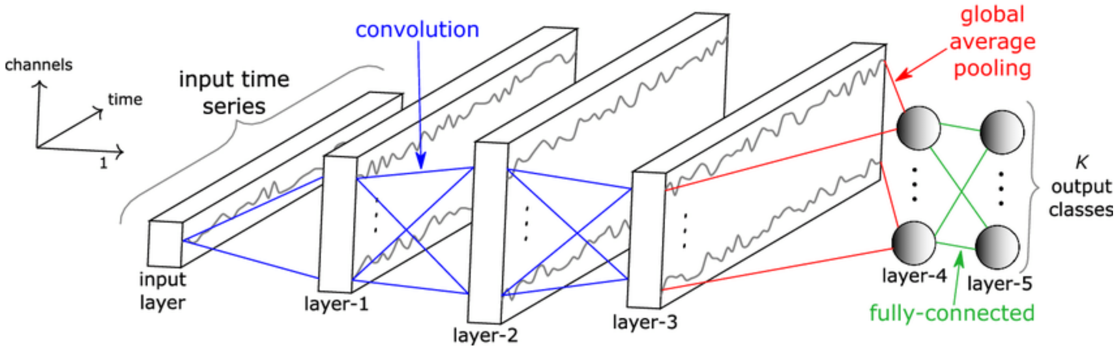

Figure 4.12: Fully convolutional neural network architecture

1. **Architecture of a CNN**

The typical architecture of a CNN consists of several layers , each fulfilling specific functions to transform input sequence of data into a meaningful output. Primary components of a CNN include:

Input Layer: This layer receives the raw input data. In the context of fault detection, this could be voltage or current signals transformed into a suitable format, such as a spectrogram or other time-series representations.

Convolutional Layers:

Convolutional filters are applied to input data through these layers. Each filter conducts a convolutional operation and traverses the input data with computed dot products to produce feature maps. The key parameters of convolutional layers include:

- Filter Size (Kernel Size): Dimensions of the convolutional filters showing the size of the receptive field.
- Stride: The size of the step that the filter moves with on the input data.
- Padding: The method of handling borders, either by adding zeros (zero padding) or without padding (valid padding).

Activation Function: The most commonly used activation function after each convolution layer used is the Rectified Linear Unit (ReLU). The ReLU makes the process nonlinear so that a very complex pattern can be captured by the network.

Pooling Layers: The pooling layer decreases the spatial dimensions of the feature maps generated by the convolution layers, in addition to reducing the computational load and the number of parameters. The most popular methods used for pooling are max pooling and average pooling.

Fully Connected Layers: These work much like the traditional neural network, in the sense that every neuron in the preceding layer is connected to each neuron in the next layer, thereby supplying high-level reasoning regarding input features.

Output Layer: . When the task at hand is a classification task, the softmax function is implemented in the output layer to make this decision on the probability distribution over target classes from the final activation.

2. **Training a CNN** Training a CNN is done in several steps to have the parameters of the network trained to their maximum:

- Forward Propagation: The first step in the model training phase where the input data is propagated through the network to compute the output.
- Loss Calculation: A loss function computes how much the predicted output deviates from the actual target output.. For classification, categorical cross-entropy is usually used.
- Backpropagation: Applying the chain rule from output to input, gradients of the loss function are calculated with respect to the weights of the network for each individual layer.

- Weight Update: The weights are updated using an optimization algorithm, such as SGD (Stochastic Gradient Descent) or its variants, by minimizing the loss.

CNNs offer several advantages for fault detection in power electronics:

- Automatic Feature Extraction: No requirement of human intervention for data preprocessing and feature extraction from raw data.
- Spatial Hierarchies of Features: CNNs learn from simple features in the initial layers to more complicated ones in the deeper layers.
- Parameter Sharing: Parameters at different spatial locations are shared by the convolutional layers, which leads to minimizing the total parameters and computational complexity.
- Translation Invariance: Due to local connectivity and pooling operations, the network allows for a certain degree of translation invariance. It is useful for making the network insensitive to slight shifts and deformations in the data.

Mathematically, the input to the model is a time series with shape $(n_{\text{timesteps}}, n_{\text{features}})$:

$$\mathbf{X} \in \mathbb{R}^{n_{\text{timesteps}} \times n_{\text{features}}} \tag{4.4.1}$$

Each convolutional layer applies a set of filters to the input:

$$y_{i,j} = \sum_{k=0}^{K-1} \sum_{m=0}^{M-1} w_{k,m}^{(j)} x_{i+k,m} + b_j \tag{4.4.2}$$

where:

- $y_{i,j}$ is the output at position i for the j-th filter.
- K is the size of the kernel filter.
- M is the length of input features.
- $w_{k,m}^{(j)}$ are the filter weights.
- b_j is the bias term.

Normalization of the output of the convolutional layer is given by equations:

$$\hat{y}_{i,j} = \frac{y_{i,j} - \mu_j}{\sqrt{\sigma_j^2 + \varepsilon}} \tag{4.4.3}$$

$$z_{i,j} = \gamma_j \hat{y}_{i,j} + \beta_j \tag{4.4.4}$$

where:

- μ_j and σ_j^2 represents the mean and variance of the activations respectively.
- Numerical stability is represented by a small constant ε.
- γ_j and β_j shows learnable parameters for scaling and shifting.

The use of ReLU activation in 1D CNNs is particularly advantageous due to its computational efficiency and its ability to allieviate the vanishing gradient problem, which can take effect due to activation functions like sigmoid and tanh. By retaining only positive values while the negative values are set to zero, ReLU facilitates faster training and convergence of the network, allowing it to effectively learn from the input data. The ReLU activation function is applied using equation 4.4.5.

$$a_{i,j} = \max(0, z_{i,j}) \tag{4.4.5}$$

Global average pooling reduces each feature map to a single value:

$$g_j = \frac{1}{n_{\text{timesteps}}} \sum_{i=0}^{n_{\text{timesteps}}-1} a_{i,j} \tag{4.4.6}$$

The dense layer with softmax activation outputs class probabilities is shown in equation 4.4.7

$$p_k = \frac{e^{z_k}}{\sum_{j=0}^{C-1} e^{z_j}} \tag{4.4.7}$$

where:

- $z_k = w_k \cdot g + b_k$
- C is the target number of classes.
- w_k and b_k are the weights and biases of the dense layer.

Table 4.1 shows a summary of the architecture that we have implemented in our research. The architecture starts with three convolutional layers. In more detail, the first convolution layer has 128 filters with a kernel size of 8, the second layer has 256 filters with a kernel size of 5, and the third one has 128 filters with a kernel size of 3. Same padding for each convolutional layer is applied to keep the input dimension. Then, we apply batch normalization and an activation function such as ReLU. A Global Average Pooling layer follows to further reduce the data dimension by averaging each feature map. Finally, a Dense layer serves as the output layer which uses a softmax activation function for finding the probability distribution over the target classes, such that it makes the fault classification possible.

For model compilation, the Adam optimizer is used while the loss function is chosen to be the categorical-cross entropy. It is trained with batch size of 128 for 100 epochs. 25% of the data is reserved for testing. The process of training is through iterative forward and backward passes into the network, in which the weights are adjusted to minimize the loss function. This iterative optimization continues until the model achieves satisfactory accuracy and loss metrics on the validation data.

Layer	Type	Parameters
1	Conv1D	Filters: 128, Kernel Size: 8, Padding: 'same', Input Shape: (X_train.shape[1], X_train.shape[2])
2	BatchNormalization	-
3	Activation	ReLU
4	Conv1D	Filters: 256, Kernel Size: 5, Padding: 'same'
5	BatchNormalization	-
6	Activation	ReLU
7	Conv1D	Filters: 128, Kernel Size: 3, Padding: 'same'
8	BatchNormalization	-
9	Activation	ReLU
10	GlobalAveragePooling1D	-
11	Dropout	0.4
12	Dense	49, Activation: Softmax

Table 4.1: CNN architecture

Long Short Term Memory

LSTM networks are a form of recurrent neural network (RNN) primarily used to be able to better capture temporal dependencies in sequential data, generally time series, as compared to its predecessors. LSTM provide superior performance and can handle various issues in temporal data as compared to traditional RNNs, particularly the problem of vanishing gradient, by introducing a unique architecture that includes memory cells and gates which regulate how the information flows through the system. The provided LSTM model architecture for time series classification includes LSTM layers to learn temporal patterns, followed by dense layers to perform the classification task.

Mathematically, LSTM cell consists of several gates that dictate how and what information flows through the network, allowing the network to maintain and update its state over time.

The forget gate (f_t) has the purpose of deciding how much information should be deleted from the prior cell state. It is computed as follows:

$$f_t = \sigma(W_f \cdot [h_{t-1}, x_t] + b_f) \tag{4.4.8}$$

where:

- σ is the activation function known as sigmoid.
- W_f are the weights for the forget gate of LSTM.
- b_f are the corresponding biases for the forget gate.
- h_{t-1} is the hidden state from the prior time step.
- x_t is the input at the current time step.

The input gate (i_t) controls how much of the incoming new and unique information must be incorporated into the cell state. It is given by:

$$i_t = \sigma(W_i \cdot [h_{t-1}, x_t] + b_i) \tag{4.4.9}$$

where:

- W_i are the weights for the input gate of LSTM.
- b_i are the biases for the input gate.

The candidate cell ($\tilde{C}_t$) state depicts the new information that can be appended to the cell state. It is calculated as:

$$\tilde{C}_t = \tanh(W_C \cdot [h_{t-1}, x_t] + b_C) \tag{4.4.10}$$

where:

- tanh is the activation function known as the hyperbolic tangent.
- W_C are the weights for the candidate cell state of LSTM.
- b_C are the biases for the candidate cell state.

The cell state (C_t) is updated by the combination OF the old cell state (modulated by the forget gate) and the new, incoming candidate values (modulated by the input gate):

$$C_t = f_t \odot C_{t-1} + i_t \odot \tilde{C}_t \tag{4.4.11}$$

where $\odot$ represents element-wise multiplication.

The output gate (o_t) is tasked with determining the output of the current cell state. It is given by:

$$o_t = \sigma(W_o \cdot [h_{t-1}, x_t] + b_o) \tag{4.4.12}$$

where:

- W_o are the weights for the output gate of LSTM.
- b_o are the biases for the output gate.

The hidden state (h_t) is computed by the following formula:

$$h_t = o_t \odot \tanh(C_t) \tag{4.4.13}$$

These equations encapsulate the core functionality of LSTM networks, enabling them to effectively model complex temporal dependencies in sequential data.

4.4.2 Bi-LSTM

Bidirectional LSTM (Bi-LSTM) is a special kind of Recurrent Neural Network (RNN) architecture that is widely applied in Machine Learning. Unlike the traditional LSTM layers, through which sequences are processed in one direction only, Bi-LSTM layers allow an input sequence to be processed in both forward and backward directions at the same time. This ability to process bidirectionally makes it possible to include information not only from the previous time steps but also from those coming next into the framework.

More formally, a Bidirectional LSTM (Bi-LSTM) layer consists of two LSTM sublayers, each of which processes an input sequence from a different direction: one forward and the other backward, as illustrated in Figure 4.13 [19]. This makes it possible for the network to incorporate information from both past and future contexts, which is highly beneficial in tasks where the complete understanding of the sequence is needed. This is very useful in such areas as natural language processing, speech recognition, and audio processing fault detection where the meaning of a given sequence may be defined based on the overall context rather than merely adjacent elements.

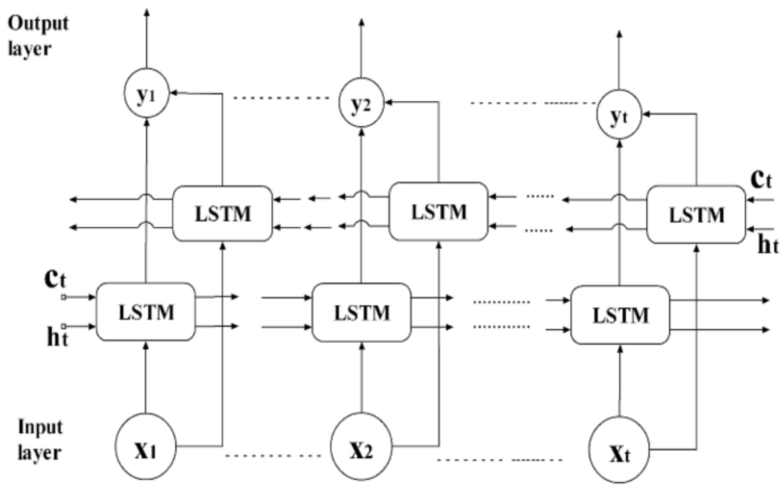

Figure 4.13: BI-LSTM architecture

The output sequences from these two LSTM sublayers are concatenated and further sent to the succeeding layer in the neural network. The concatenated output presents a significantly deeper insight into the sequence, in which information from both past and future directions is combined. This property enhances the model's capability of learning dependencies and patterns in sequential data, thereby making it more relevant for applications that require sensitive understanding and prediction across time.

In the current research, the input layer of the Bi-LSTM model considers a sequence of 7590 timesteps, where each timestep accommodates 3 features. This layer is important in that it ensures the model perceives properly the structure of the time series data, leading to proper learning influence brought about by the sequences.

The first hidden layer in our model IS a bidirectional LSTM with 128 units. Bidirectional allows dependencies to be captured not only in the forward but also in the backward directions, which improves the model's ability to decipher complex temporal relationships. In addition, to prevent overfitting, a dropout layer with a dropout rate of 0.3 is used. The purpose of the batch normalization is to stabilize and speed up the training by normalizing the outputs of the LSTM layer.

The second layer is bidirectional LSTM Layer with Dropout and batch normalization. This hidden layer also follows the first hidden layer's structure. It also uses a bidirectional LSTM containing 128 units. This layer, in turn, increases the capacity of the model to capture complex patterns of the data. Similar to the previous layer, a dropout layer is also added to reduce overfitting and batch normalization to stabilize and accelerate training.

The third hidden layer further reduces the LSTM units to 64 to now make it even more compressed in its representation of learned features. This reduction is done to abstract the necessary patterns out of data while keeping the bidirectionality for a holistic temporal learning process. In the same way as for previous layers, dropout and batch normalization are used here to reinforce generalization and boost training efficiency.

Lastly, the output layer of the model: this dense layer consists of 49 neurons, each corresponding to one of the 49 classes in our classification task. The softmax function is used on the output layer, allowing it to give a probability distribution over the 49 classes so that the model can output confident predictions for each input sequence. The architecture is shown in table 4.2

Layer	Type	Parameters
1	InputLayer	Input Shape: (7590, 3)
2	Bidirectional LSTM	Units: 128, Return Sequences: True, Kernel Regularizer: L2(0.001)
3	Dropout	Rate: 0.3
4	BatchNormalization	-
5	Bidirectional LSTM	Units: 128, Return Sequences: True, Kernel Regularizer: L2(0.001)
6	Dropout	Rate: 0.3
7	BatchNormalization	-
8	Bidirectional LSTM	Units: 64, Kernel Regularizer: L2(0.001)
9	Dropout	Rate: 0.3
10	BatchNormalization	-
11	Dense	Units: 49, Activation: Softmax

Table 4.2: Bi-LSTM architecture

4.4.3 CNN-LSTM

A hybrid CNN-LSTM model leverages the strengths of CNN as well as the LSTM networks. The CNN-LSTM architecture embodies the feature extraction capabilities of CNNs and combines it with the sequential learning strengths of LSTM networks. This hybrid approach is particularly effective for time-series classification tasks, such as fault detection in solar-fed multi-level inverters. Here's a detailed explanation of the CNN-LSTM architecture and its application in this context.

1. **CNN**:

   - Feature Extraction: CNNs are powerful neural networks which are adept at extracting spatial features from input data. They extract features from the input sequence by applying convolutional filters, which helps in capturing local patterns and hierarchical features.
   - Layers: Typical CNN layers include convolutional layers which are the primary source of feature extraction, activation functions (like ReLU, Tanh) for inducing non-linearity, pooling layers for mininizing computational complexity, and sometimes batch normalization.

2. **LSTM Networks**:

   - Sequential Learning: LSTM networks, a type of recurrent neural network (RNN), excel at learning long-term dependencies in sequential data. They are adept at capturing temporal patterns and contextual information in time-series data.

Table 4.3 shows the architecture designed to detect faults in a 5-level CHB inverter system powered by solar energy. The model uses CNN layers for initial feature extraction followed by LSTM layers for capturing temporal dependencies.

The architecture begins with an input of sequence data and has a one-dimensional convolutional layer with 64 filters applied to it, having a kernel size of 3, which is meant to extract local patterns in the input sequence data. It then processes the output using the ReLU activation function in order to introduce non-linearity. After the convolutional layer, a MaxPooling1D layer is applied on the data. It has a pool size of 2 in order to reduce the spatial data dimension, summarizing feature representation with some form of translation invariance.

The extracted features from the CNN are then passed through an LSTM layer with 100 neurons aimed at capturing temporal dependencies in sequential data. This architecture layer enabled

Layer	Type	Parameters
1	Input Layer	Shape: (timesteps, features)
2	Conv1D	Filters: 64, Kernel Size: 3, Activation: ReLU, Input shape: (7590, 3)
3	MaxPooling1D	Pool Size: 2
4	LSTM	Units: 100, Return sequences: False
5	Dense	Units: 100, Activation: ReLU
6	Dropout	Rate: 0.5
7	Dense	Units: num_classes, Activation: Softmax

Table 4.3: CNN-LSTM architecture

processing of time series data and learning long-term dependencies in such a way that the temporal context of the data was properly defined. In this case, further transformation of the features learned by LSTM has been carried out following the LSTM layer using a dense layer employing 100 neurons with the ReLU activation function.

We integrate a dropout layer of rate 0.5 for the reduction of overfitting. During training, the neurons in the dropout layers are randomly dropped so that the model does not rely heavily on specific paths. At the end, we add a dense layer with 49 neurons. We apply a softmax activation function to this layer so as to get probability distributions over the classes.

4.4.4 Residual network

ResNet revolutionized the world of deep learning by rectifying the vanishing gradient problem, which often hampers the training of neural networks with many layers. Introduced by Kaiming He et al. in their 2015 paper titled "Deep Residual Learning for Image Recognition," ResNet enables the training of extremely deep networks by using a novel architectural feature called "residual blocks."[12]

Vanishing Gradient Problem Vanishing gradient is a problem in which, in deep networks, gradients can become exceedingly small, preventing the network from effectively updating weights and learning. This issue often limits the depth of traditional neural networks.

Residual Learning The core idea of ResNet is residual learning. Instead of each layer learning a direct mapping from input to output, the layer learns the residual. The residual is the difference between the input and the desired output as shown in figure 4.14. Formally, the network does not learn $H(x)$, rather it learns $F(x) = H(x) - x$, where $H(x)$ is the original function and x is the input. The original function then becomes $H(x) = F(x) + x$.

Residual Block A residual block typically consists of two or three layers. The input x is propogated through the layers to produce $F(x)$, and then x is added to $F(x)$ before applying the activation function. Mathematically, it can be expressed as:

$$y = F(x, \{W_i\}) + x \tag{4.4.14}$$

where y is the block's output, W_i represents the weights of the layers, and $F(x, \{W_i\})$ is the residual mapping.

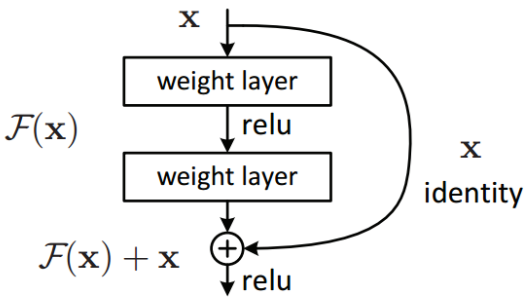

Figure 4.14: Residual connection

Skip Connections: These are shortcuts that skip one or more layers, and instead connect the input of the residual block directly to its output block. Skip connections help alleviate the vanishing gradient problem by enabling gradients to flow directly through the network, even when they become very small.

Network Depth: ResNet architectures are denoted as ResNet-50, ResNet-101, ResNet-152, etc., where the number denotes how many layers constitute the network. This deep architecture is made feasible by the use of residual blocks.

Batch Normalization: Batch normalization is employed after each convolutional layer and before the activation function within the residual blocks. It normalizes the output of each layer, thus allowing the training process to be stabilized and also accelerated.

Activation Function: Typically, ReLU (Rectified Linear Unit) serves as the activation function in ResNet. It introduces non-linearity into the network, facilitating the learning of intricate patterns.

Identity vs. Convolutional Blocks:

- Identity Blocks: These blocks perform identity mapping, i.e., the dimensions are the same for both the input and output.
- Convolutional Blocks: These blocks change the input's dimensions using convolution layers with stride greater than 1 or through pooling.

Global Average Pooling: Rather than using fully connected layers, ResNet often utilizes global average pooling at the end of the network. This technique cuts down the spatial dimensions of the feature maps to a single vector per feature map, helping to mitigate overfitting and reducing computational load.

Mathematical Formulation: Residual Function:

$$F(x) = \mathrm{ReLU}(\mathrm{BN}(W_2 \cdot \mathrm{ReLU}(\mathrm{BN}(W_1 \cdot x)))) \tag{4.4.15}$$

Here, W_1 and W_2 are weights of layers of convolution, BN denotes batch normalization, and ReLU serves as the activation function.

Output of Residual Block: :

$$y = F(x) + x \tag{4.4.16}$$

In the bottleneck architecture: **Bottleneck Residual Function:**

$$F(x) = W_3 \cdot \mathrm{ReLU}(\mathrm{BN}(W_2 \cdot \mathrm{ReLU}(\mathrm{BN}(W_1 \cdot x)))) \tag{4.4.17}$$

Here, W_1, W_2, and W_3 are weights of the convolutional layers, and the convolutions are typically 1x1, 3x3, and 1x1 respectively.

Advantages of ResNet

- Ease of Training: By using residual learning, ResNet mitigates the vanishing gradient problem, making it feasible to train much deeper networks.
- High Accuracy: ResNet models have achieved state-of-the-art results on many benchmark tasks, such as image classification and object detection.
- Flexibility: The architecture can be easily adapted for various tasks and extended to very deep networks.

In summary ResNets leverage the idea of residual learning, which assists in mitigating the problem of vanishing gradient (where gradients become so small they approach zero and thus no learning occurs) problem which is often seen in deep neural networks. The core functionality of ResNet is the residual block, which allows the network to learn residual functions correspondning to the layer inputs, instead of learning them via unreferenced functions. The provided ResNet model is designed with 1D convolutional layers tailored for time series data. Each residual block has the following architecture: convolutional layers, which are then followed by batch normalization and finally by the ReLU activation as shown in 4.15 [14].

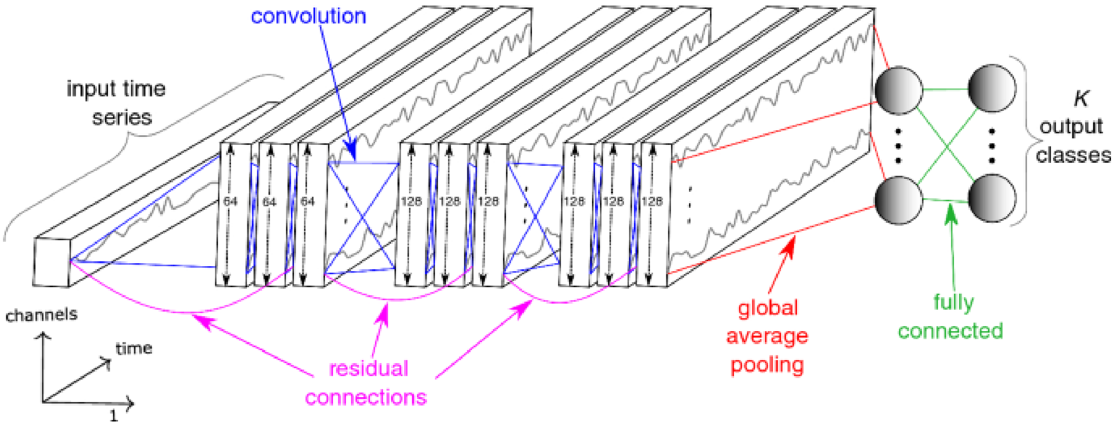

Figure 4.15: ResNet architetcure

The ResNet architecture in our research starts with an initial convolutional layer, followed by batch normalization and ReLU activation function for induction of non-linearity. The model then includes a sequence of residual blocks, each composed of two convolutional layers with batch normalization and ReLU activation function. The first block in each series optionally includes a convolutional shortcut connection to match the dimensions when the number of filters changes. Specifically, the architecture includes three groups of residual blocks with increasing filter sizes (64, 128, and 256), which progressively capture more complex features. The output from the last residual block is globally averaged and passed through a dense layer with a softmax activation to produce the final classification output, making the model suitable for identifying different types of switch faults in H-bridge multilevel inverters. Table 4.4 captures the essential details of each layer in the ResNet architecture in our research, including the output shape, number of parameters, and specific details about the layer configuration.

Layer Type	Output Shape	Param #
Input Layer (*InputLayer*)	(None, 7590, 3)	0
Conv1D (*conv1d*)	(None, 7590, 64)	1600
BatchNormalization	(None, 7590, 64)	256
Activation (*ReLU*)	(None, 7590, 64)	0
Residual Block 1	(None, 7590, 64)	-
Residual Block 2	(None, 7590, 128)	-
Residual Block 3	(None, 7590, 256)	-
GlobalAveragePooling1D	(None, 256)	0
Dropout	(None, 256)	0
Dense	(None, 49)	12593

Table 4.4: ResNet architecture

Parameter Calculation

Understanding the number of parameters in each layer of a neural network is crucial for analyzing its complexity and performance. Below, we provide the detailed calculations for the parameters of the Conv1D, BatchNormalization, and Dense layers.

Conv1D Layer

The parameters for a Conv1D layer are calculated using the formula:

$$\text{Params} = (\text{kernel size} \times \text{input channels} \times \text{filters}) + \text{filters}$$

For our Conv1D layer:

$$\text{Params} = (8 \times 3 \times 64) + 64 = 1600$$

BatchNormalization Layer

The parameters for a BatchNormalization layer are calculated using the formula:

$$\text{Params} = 4 \times \text{filters}$$

For our BatchNormalization layer:

$$\text{Params} = 4 \times 64 = 256$$

Dense Layer

The parameters for a Dense layer are calculated using the formula:

$$\text{Params} = (\text{input units} \times \text{output units}) + \text{output units}$$

For our Dense layer:

$$\text{Params} = (256 \times 49) + 49 = 12,593$$

4.5 Conclusion

In this chapter, we have delved into the methodologies and deep learning architectures employed for fault detection in solar-fed 5-level CHB inverter. We began with an introduction to data collection and preprocessing techniques, emphasizing the importance of handling real-world data variability and noise. The inclusion of WGN into voltage signals was discussed at length, and its criticality emphasized to simulate practical scenarios, which further made the model robust against varied noise levels.

We also summarized some deep learning techniques in detail so that the role of each type in fault detection is clearly understood. With this in mind, comprehensive details of the FCN, Bi-LSTM, CNN-LSTM, and ResNet architectures were elaborated on in respect to their structural elements, mathematical underpinnings, and particular advantages. The summarized findings were presented in a comparative table that placed specific emphasis on architecture differences and their relevance to fault detection performance.

In general, this chapter has provided a solid base to understand technical complexities and practical applications of advanced neural network architectures toward the performance, reliability, and efficiency improvement of any developed fault detection system. These are important insights to help promote resilient renewable energy systems and ensure optimal performance, including minimizing downtime. The subsequent chapters will go into this in more detail and explain the practical application and testing of the models in a real-world scenario.

CHAPTER 5

Results and Discussion

The chapter demonstrates the performance and effectiveness of the developed neural network architectures for fault detection in renewable energy systems. Empirical results obtained from the training and testing of each model will be presented, followed by a critical analysis and interpretation of the results. The discussion is held in view of the research objectives to present insights into the performance of the model, robustness, and suitability for application in the real world.

5.1 Performance evaluation metrics

The performance of models in the field of fault detection of renewable energy systems using neural networks is measured through the application of rigorous metrics of assessment. The importance of these metrics is very high in quantifying the accuracy, reliability, and robustness of the model in detecting faults in different operational conditions. It's in this section that we delve into key performance metrics that play pivotal roles in the effectiveness of neural network models:

Accuracy

Accuracy is the most basic metric that tells how correct a model's prediction is. Mathematically, it is defined in 5.1.1.

$$\text{Accuracy} = \frac{\text{No. of Correct Predictions}}{\text{Total No. of Predictions}} \tag{5.1.1}$$

While accuracy gives an overall view of how a model is performing, it is not sufficient when class distributions are imbalanced.

Precision

Precision gauges how accurate the positive predictions of the model are close to being accurate. It evaluates whether the model sidesteps the mistake of labeling data points as being positive that is not true. It can be determined using equation 5.1.2.

$$\text{Precision} = \frac{\text{True Positives}}{\text{True Positives + False Positives}} \tag{5.1.2}$$

Precision is important in applications where misclassification of positives can have serious consequences.

Recall (Sensitivity)

Recall is measure of the model's ability to capture most of the positive samples out of the actual number of positives present in the dataset. It is calculated as:

$$\text{Recall} = \frac{\text{True Positives}}{\text{True Positives + False Negatives}} \tag{5.1.3}$$

This is important, in particular, for applications where false negatives (missing positive instances) are undesirable.

F1-score

A harmonic mean of precision and recall is given by the F1 score. Hence it is a metric that gives a balanced measure of the model's performance.

$$\text{F1-score} = 2 \times \frac{\text{Precision} \times \text{Recall}}{\text{Precision + Recall}} \tag{5.1.4}$$

Therefore, useful measures for case classes with imbalanced distribution should provide very comprehensive measures of model effectiveness.

Confusion Matrix

A table that is used to describe the performance of a classification model on the set of test data is called confusion matrix; it results in counts of the correct and incorrect positive items. It highlights in detail where a model does well or struggles to predict something.

These metrics collectively serve as crucial benchmarks for evaluating neural network models designed for fault detection in renewable energy systems. They enable researchers and engineers to quantify the performance of their models accurately, identify strengths and weaknesses, and guide further refinements for enhanced real-world applications.

5.2 Training and validation performance

The ResNet model demonstrates robust learning and generalization capabilities, as evidenced by the accuracy and loss plots in figure 5.1. The initial rapid improvements followed by stabilization are typical in well-trained deep learning models. The fluctuations in validation accuracy and loss are common and reflect the inherent variability in the validation data set. The overall trends suggest that the ResNet model effectively learns the underlying patterns associated with switch faults in PV systems. The high final validation accuracy, coupled with the low validation loss, indicates strong generalization to unseen data, reaffirming ResNet's suitability for this fault detection task. It can be seen that the accuracy has an exponential growth in the earlier epochs and then plateaus at higher epochs. Similarly, the loss is reduced exponentially at the start and stabilizes at higher epochs.

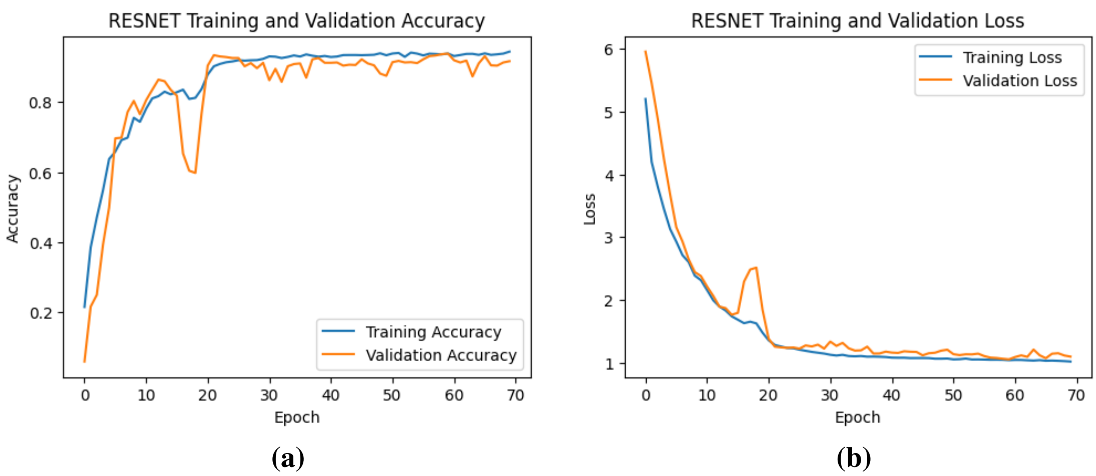

Figure 5.1: (a) Accuracy for training and validation sets and (b) Loss for training and validation sets of ResNet

Other models performance on validation and training data for 0db is shown in figures 5.2 ,5.3 and 5.4. For the LSTM model, we can see that the accuracy sharply increases till about 40 epochs then suffers for about 20 epochs with the accuracy flip flopping until it stabilizes at around 70 percent. However, it then suffers a decline at higher epochs, suggesting that optimum accuracy peaks at around 90 epochs and then suffers a downturn. The loss follows a similar pattern in the opposite direction.

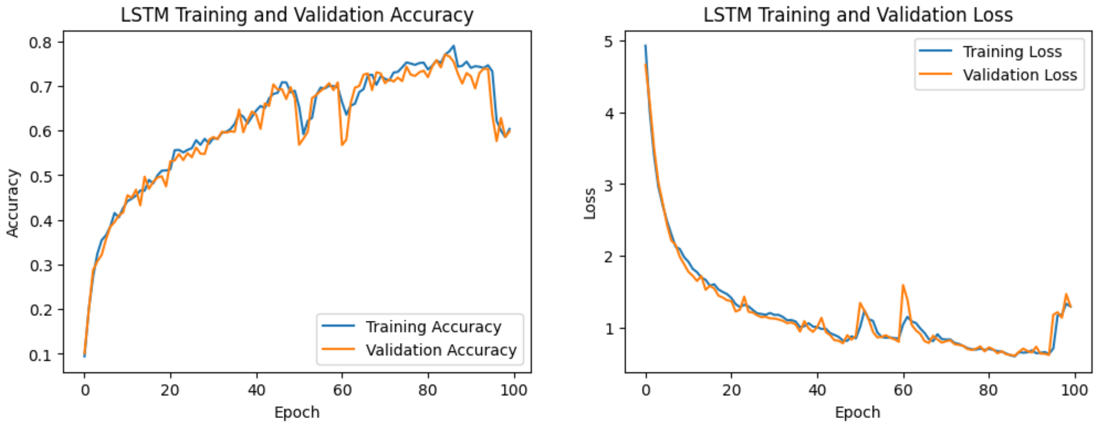

(a) **(b)**

Figure 5.2: (a) Accuracy for training and validation sets and (b) Loss for training and validation sets of LSTM

The fully connected convolutional model performs at a more general pattern, increasing exponentially till about 40 epochs and then settling at around 80 percent accuracy for the complete 100 epochs. The loss also follows a similar pattern, by decreasing exponentially and then stabilizing from 40 epochs onwards, to about 0.5 as shown in figure 5.3. Compared to LSTM, it has a much smoother training process.

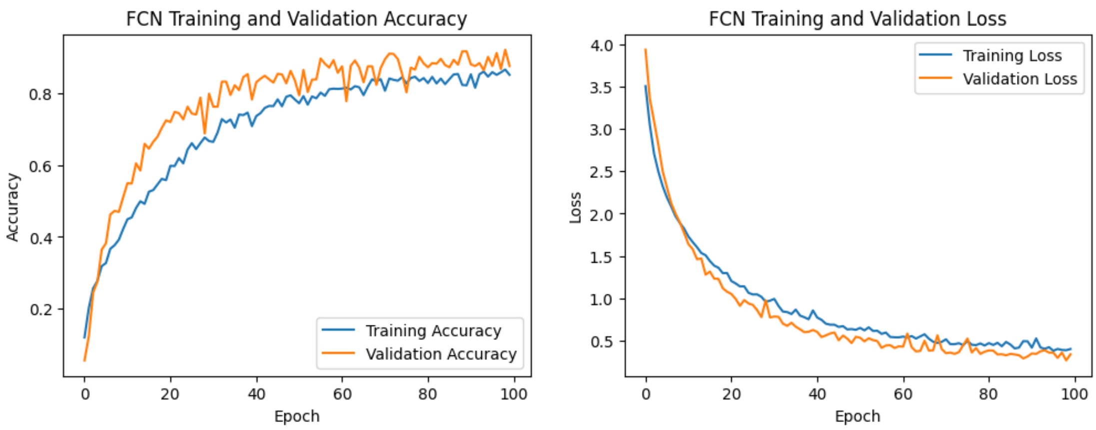

(a) **(b)**

Figure 5.3: (a)Accuracy for training and validation sets and (b) Loss for training and validation sets of FCN

Finally, we have the CNN-LSTM hybrid model. This performs similarly to the fully connected neural network model, albeit with even lesser ups and downs as shown in 5.4. The model also reaches a peak accuracy of about 80 percent, with the loss being reduced to about 0.5.

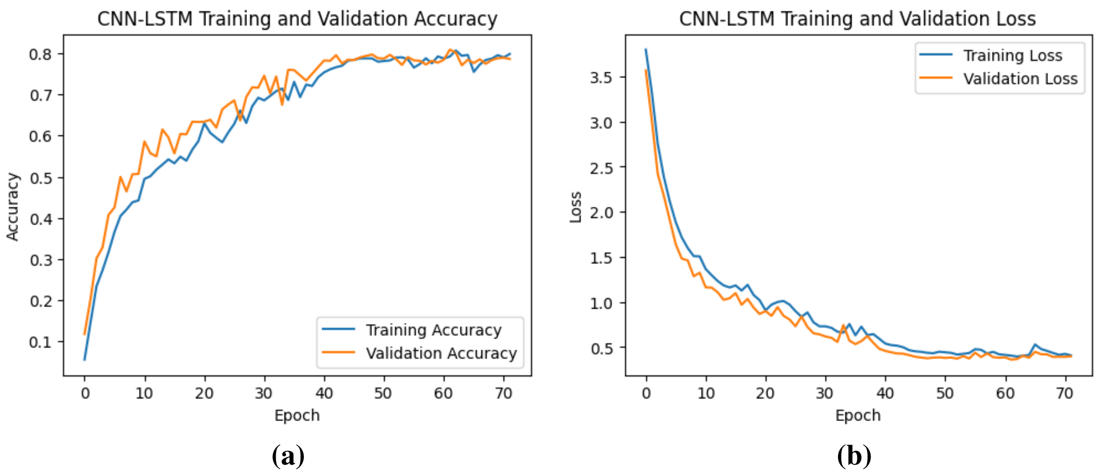

Figure 5.4: (a) Accuracy for training and validation sets and (b) Loss for training and validation sets of CNN-LSTM

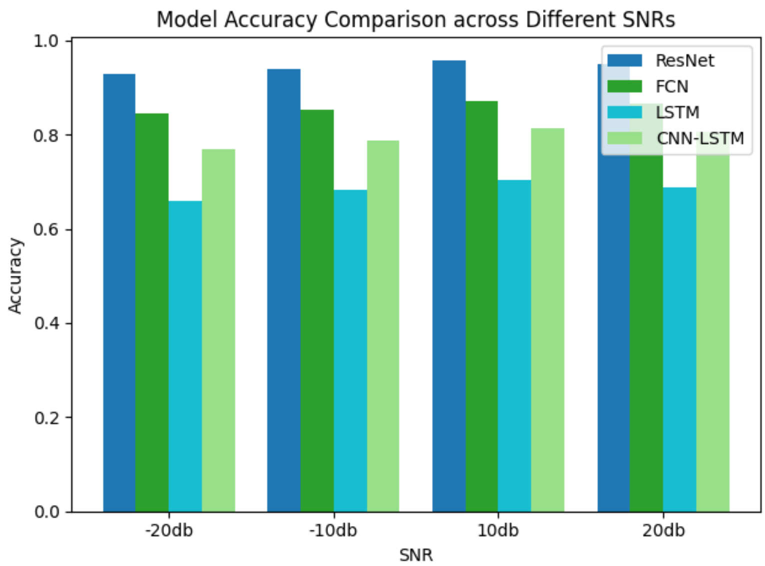

Figure 5.5: Models comparison of accuracy across different SNR

The comparative performance of accuracy for all SNRs is shown in figure 5.5. The figure clearly indicate that ResNet is the most effective model for detecting switch faults in PV fed 5 level CHB inverter. Its superior accuracy underscore its robustness and reliability in real-world applications.

5.3 Comparitive analysis across different SNR

These metrics present vital benchmarks through which the neural network models can be judged and compared among themselves for fault detection in renewable energy systems. They further make it possible to compare performance on different models at varying SNR levels. These SNR levels are -20 dB, -10 dB, 0 db, 10 dB, and 20 dB. The results are presented in table 5.1. The high scores across all metrics in table 5.1 suggest that ResNet can effectively distinguish between faulty and non-faulty states with minimal errors, making it highly suitable for practical implementation in fault detection systems. The FCN model, while not as effective as ResNet, still shows reasonably good performance and could be considered a viable alternative in scenarios where computational resources are constrained, given its relatively simpler architecture compared to ResNet. On the other hand, the CNN-LSTM and LSTM models, with their comparatively lower performance metrics, might require further optimization or could be used in conjunction with other methods to improve their fault detection capabilities.

The performance of these algorithms has been evaluated with the key performance metrics, which cover all aspects of evaluation: accuracy, precision, recall, and F1-Score. These clearly presented the performance of different approaches for accurate fault detection of switches in the solar-powered cascaded H-bridge inverter under differing levels of white Gaussian noise.

Analysis of results

1. Accuracy:

Consistently achieves the highest accuracy across all SNR levels, pointing out its robustness in fault detection tasks. At -20 dB SNR, the accuracy achieved by ResNet was 92.93%, which is better than the values for FCN (84.39%), LSTM (65.89%), and CNN-LSTM (76.93%). Such a trend proceeds for the rest of the levels, with ResNet dominating or sharing levels of top accuracy in across all noise levels.

2. Precision:

Precision shows how well the model has predicted the actual positive instances among all the predicted positive instances. ResNet still outperforms other models at all the SNR levels. In fact, even at -20 dB SNR, the precision of ResNet is 93.60% compared to that of FCN (87.88%), LSTM (68.15%), and CNN-LSTM (76.16%). The trend shows that ResNet effectively reduces false positives. The precision of ResNet for other levels is 94% for -10 db and around 95% for

SNR (dB)	Metric	FCN	LSTM	CNN-LSTM	ResNet
-20	Accuracy	0.8439	0.6589	0.7693	0.9293
	Precision	0.8788	0.6815	0.7616	0.9360
	Recall	0.8439	0.6589	0.7693	0.9293
	F1-score	0.8326	0.6476	0.7423	0.9266
-10	Accuracy	0.8526	0.6826	0.7888	0.9406
	Precision	0.8790	0.6989	0.8008	0.9423
	Recall	0.8526	0.6826	0.7888	0.9406
	F1-score	0.8418	0.6689	0.7767	0.9397
0	Accuracy	0.8711	0.6801	0.8009	0.9483
	Precision	0.8910	0.6917	0.8091	0.9491
	Recall	0.8711	0.6801	0.8009	0.9483
	F1-score	0.8626	0.6662	0.7887	0.9479
10	Accuracy	0.8711	0.7040	0.8134	0.9587
	Precision	0.8943	0.7236	0.8287	0.9593
	Recall	0.8711	0.7040	0.8134	0.9587
	F1-score	0.8605	0.6929	0.8040	0.9585
20	Accuracy	0.8666	0.6875	0.8051	0.9510
	Precision	0.8892	0.7040	0.8120	0.9517
	Recall	0.8666	0.6875	0.8051	0.9510
	F1-score	0.8561	0.6764	0.7931	0.9506

Table 5.1: Performance metrics for models across various SNR levels

10 and 20 db.

3. F1-score:

The F1-score for combining the overall scores of precision and recall highlights once more the steady performance of ResNet. In this case, F1-scores on ResNet at various SNR levels are robust and are indicative of balanced performance between precision and recall. For example, at -20 dB SNR, ResNet behaves with an F1-score of 92.66%, whereas FCN results in 83.26%; LSTM, 64.76%; and CNN-LSTM, 74.23%.

Comparison Across Architectures

ResNet emerged as the best-performing model with a fault detection time of 0.07s, consistently achieving the highest accuracy, precision, recall, and F1 score across all SNR levels. Its architecture, including residual connections, effectively mitigates the vanishing gradient problem, allowing the network to learn deep, intricate patterns within the data. This capability proved particularly valuable in accurately distinguishing fault conditions from normal operations, even in noisy environments. FCN ranked second, delivering strong results, especially in less noisy environments, due to its simplicity and ability to capture global features, though it struggled with higher noise levels. CNN-LSTM showed moderate performance; its hybrid architecture leveraged CNNs for spatial learning and LSTMs for temporal dynamics, but it did not outperform ResNet or FCN, possibly due to complexity and overfitting issues. LSTM was the least effective, with the lowest performance metrics and longest training time, struggling with spatial feature capture and sensitivity to noise. Increasing noise levels negatively impacted all models, but ResNet maintained superior performance, highlighting the importance of model selection in fault detection within PV systems under varying noise conditions.

5.4 Limitations

1. **Dataset Size and Diversity:** The study's reliance on a specific dataset, though extensive, may limit the generalizability of findings to broader contexts. The dataset used primarily represents a specific geographic area or operational conditions, potentially overlooking variations in environmental factors or equipment configurations that could affect fault detection performance in different settings.

2. **SNR Variation and Real-world Conditions:** While the study evaluated model performance across different Signal-to-Noise Ratio (SNR) levels, the simulated noise conditions may not fully capture the complexities of real-world environments. Variations in noise characteristics and dynamic operational conditions (e.g., rapid weather changes affecting solar energy output) could influence the models differently than simulated scenarios.

3. **Architecture-Specific Considerations:** Each neural network architecture (FCN, LSTM, CNN-LSTM, ResNet) comes with its own strengths and limitations. For instance, while ResNet demonstrated superior performance in most metrics, its computational complexity

and training requirements may pose practical challenges in resource-constrained environments compared to simpler architectures like FCN.

4. **Validation and Overfitting:** Although efforts were made to mitigate overfitting through cross-validation and regularization techniques, the potential for overfitting to specific characteristics of the training dataset remains a concern. Validation across independent datasets or real-time deployment scenarios would provide further insights into model robustness and generalizability.

5.5 Conclusion

ResNet emerges as the most effective architecture for fault detection in the context of renewable energy systems, demonstrating superior accuracy, precision, and F1-score across varying SNR levels. Its residual learning approach and deep architecture enable it to capture complex patterns effectively, making it well-suited for real-world applications where robust fault detection is crucial. LSTM and CNN-LSTM show competitive performance, suitable for scenarios where computational efficiency and sequential data processing are paramount, albeit with varying strengths in different SNR conditions. FCN, while simpler in structure, shows lower overall performance compared to the other architectures evaluated here.

CHAPTER 6

Conclusion

The pursuit of efficient and reliable fault detection in switches within PV systems is crucial for the stability and longevity of renewable energy systems. This study evaluated the effectiveness of four deep learning models FCN, Bi-LSTM, ResNet, and CNN-LSTM in detecting faults under different noise levels.

Among these models, ResNet stood out as the best performer, achieving a fault detection time of just 0.07 seconds and consistently high scores in accuracy, precision, recall, and F1 across all SNR levels. Its architecture, with residual connections, effectively overcomes the vanishing gradient problem, enabling the network to learn complex patterns in the data, even in noisy conditions. FCN came in second, delivering strong results, particularly in environments with less noise. Its simplicity and ability to capture broad features made it reliable for fault detection, though it struggled more as noise increased.

CNN-LSTM showed moderate success, utilizing both CNNs for spatial learning and LSTMs for temporal dynamics, but it did not outperform ResNet or FCN, possibly due to its complexity and risk of overfitting. Bi-LSTM was the least effective, showing the lowest performance metrics and requiring the longest training time. This was likely due to its difficulty in capturing spatial features and sensitivity to noise, which disrupted its ability to detect sequential patterns. As expected, all models' performances were negatively impacted by higher noise levels, but ResNet maintained superior performance, highlighting its robustness. This research underscores the importance of choosing the right model for fault detection in PV systems, particularly under varying noise conditions. The findings suggest that models like ResNet, capable of deep feature extraction, are particularly well-suited for this task.

6.1 Future work

To address these limitations of this research, future research could focus on:

- **Diverse dataset collection:** Incorporating datasets from varied geographical locations and operational conditions to enhance model robustness and generalizability.
- **Real-time validation:** Conducting field tests or deploying models in operational settings to validate performance under real-world conditions.
- **MPPT algorithm:** Explore other algorithm for tracking maximum point from PV panel such as fuzzy logic using neural network.
- **Model explainability:** Integrating interpretability tools or developing hybrid models that balance performance with transparency, enhancing trust in AI-driven decision-making processes.
- **Other faults:** Proposing models for other types of fault such as thermal faults and upto two short circuit fault diagnosis for CHBMLIs.

By acknowledging and addressing these limitations, future studies can build upon current findings to further advance fault detection systems in renewable energy applications.

References

[1] Ezzidin Aboadla et al. “Effect of modulation index of pulse width modulation inverter on Total Harmonic Distortion for Sinusoidal”. In: Jan. 2016, pp. 192–196. DOI: 10.1109/INTELSE.2016.7475119.

[2] Damoun Ahmadi et al. “A Universal Selective Harmonic Elimination Method for High-Power Inverters”. In: *IEEE Transactions on Power Electronics - IEEE TRANS POWER ELECT* 26 (Oct. 2011), pp. 2743–2752. DOI: 10.1109/TPEL.2011.2116042.

[3] Murad Ali et al. “Open switch fault diagnosis of cascade H-bridge multi-level inverter in distributed power generators by machine learning algorithms”. In: *Energy Reports* 7 (2021), pp. 8929–8942. ISSN: 2352-4847. DOI: https://doi.org/10.1016/j.egyr.2021.11.058. URL: https://www.sciencedirect.com/science/article/pii/S2352484721012038.

[4] Anjali Anand et al. “Open switch fault detection in Cascaded H-Bridge Multilevel Inverter using normalised mean voltages”. In: *2016 IEEE 6th International Conference on Power Systems (ICPS)*. 2016, pp. 1–6. DOI: 10.1109/ICPES.2016.7584128.

[5] M.T. Benchouia et al. “Implementation of adaptive fuzzy logic and PI controllers to regulate the DC bus voltage of shunt active power filter”. In: *Applied Soft Computing* 28 (2015), pp. 125–131. ISSN: 1568-4946. DOI: https://doi.org/10.1016/j.asoc.2014.10.043. URL: https://www.sciencedirect.com/science/article/pii/S1568494614006176.

[6] Abdelkader Azzeddine Bengharbi et al. “Open-Circuit Fault Diagnosis for Three-Phase Inverter in Photovoltaic Solar Pumping System Using Neural Network and Neuro-Fuzzy Techniques.” In: *Electrica* 23.3 (2023), pp. 505–516.

[7] Fernando Bento and A.J.M. Cardoso. “A comprehensive survey on fault diagnosis and fault tolerance of DC-DC converters”. In: Vol. 4 (Sept. 2018), pp. 1–12. DOI: 10.23919/CJEE.2018.8471284.

[8] Merlin Chai, Naga Brahmendra Yadav Gorla, and Sanjib Kumar Panda. “Fault detection and localization for cascaded H-bridge multilevel converter with model predictive control”. In: *IEEE Transactions on Power Electronics* 35.10 (2020), pp. 10109–10120.

[9] Dhupchhaya Chowdhury et al. “Wavelet decomposition based fault detection in cascaded H-bridge multilevel inverter using artificial neural network”. In: *2017 2nd IEEE International Conference on Recent Trends in Electronics, Information & Communication Technology (RTEICT)*. IEEE. 2017, pp. 1931–1935.

[10] R Fazai et al. “Machine learning-based statistical testing hypothesis for fault detection in photovoltaic systems”. In: *Solar Energy* 190 (2019), pp. 405–413.

[11] Abdalmula Gebreel. “SIMULATION AND IMPLEMENTATION OF TWO-LEVEL AND THREE-LEVEL INVERTERS BY MATLAB AND RT-LAB”. PhD thesis. Mar. 2011. DOI: 10.13140/RG.2.2.35370.72649.

[12] Kaiming He et al. *Deep Residual Learning for Image Recognition*. 2015. arXiv: 1512.03385 [cs.CV]. URL: https://arxiv.org/abs/1512.03385.

[13] B Hemanth Kumar et al. “Fault Tolerant Operation of CHB Multilevel Inverters Based on the SVM Technique Using an Auxiliary Unit”. In: *Journal of Power Electronics* 18 (Jan. 2018), pp. 56–69. DOI: 10.6113/JPE.2018.18.1.56.

[14] Hassan Ismail Fawaz et al. “Deep learning for time series classification: a review”. In: *Data Mining and Knowledge Discovery* 33 (July 2019). DOI: 10.1007/s10618-019-00619-1.

[15] Madhab Jena. “"Optimization of solar power generation efficiency using MINITAB software"”. In: (Feb. 2015), p. 2.

[16] Sung Kim et al. “Recent Advances of Artificial Intelligence in Manufacturing Industrial Sectors: A Review”. In: *International Journal of Precision Engineering and Manufacturing* 23 (Nov. 2021). DOI: 10.1007/s12541-021-00600-3.

[17] Xiaoxia Li et al. “Intelligent fault pattern recognition of aerial photovoltaic module images based on deep learning technique”. In: *J. Syst. Cybern. Inf* 16 (2018), pp. 67–71.

[18] Benyettou Loutfi. “Faults detection and diagnosis of multilevel inverter based on signal processing”. In: *Traitement du Signal* 6.1 (2019), pp. 37–44.

[19] Tejas Maniar. “Application of DC-DC Converter for Grid Connected Inverter using PV Cell”. In: *Journal of Electrical Systems* 20 (May 2024), pp. 2613–2620. DOI: 10.52783/jes.4097.

[20] Pandav Kiran Maroti et al. “The state-of-the-art of power electronics converters configurations in electric vehicle technologies”. In: *Power Electronic Devices and Components* 1 (2022), p. 100001. ISSN: 2772-3704. DOI: https://doi.org/10.1016/j.pedc.2021.100001. URL: https://www.sciencedirect.com/science/article/pii/S2772370421000018.

[21] Amina Mimouni et al. “Fault diagnosis of power converters in a grid connected photovoltaic system using artificial neural networks”. In: *Electrical Engineering & Electromechanics* 1 (2023), pp. 25–30.

[22] Parvin Moamaei, Hamid Mahmoudi, and Reza Ahmadi. “Fault-tolerant operation of cascaded H-Bridge inverters using one redundant cell”. In: *2015 IEEE Power and Energy Conference at Illinois (PECI)*. 2015, pp. 1–5. DOI: 10.1109/PECI.2015.7064923.

[23] Sheik Mohammed Sulthan and D. Devaraj. *Simulation and Analysis of Stand-alone Photovoltaic System with Boost Converter using MATLAB/Simulink*. Aug. 2015.

[24] Muhammed Ramees Mullali Kunnontakath Puthiyapurayil et al. “A review of open-circuit switch fault diagnostic methods for neutral point clamped inverter”. In: *Electronics* 11.19 (2022), p. 3169.

[25] David Nilsson. *Fault detection in photovoltaic systems*. 2014.

[26] Kedar Potdar, Taher S Pardawala, and Chinmay D Pai. “A comparative study of categorical variable encoding techniques for neural network classifiers”. In: *International journal of computer applications* 175.4 (2017), pp. 7–9.

[27] Dezso Sera et al. “On the Perturb-and-Observe and Incremental Conductance MPPT Methods for PV Systems”. In: *IEEE Journal of Photovoltaics* 3 (July 2013), pp. 1070–1078. DOI: 10.1109/Jphotov.2013.2261118.

[28] Mahmoud Shahbazi and MohammadReza Zolghadri. “Fast detection of open-switch fault in cascaded H-Bridge multilevel converter”. In: *The 6th Power Electronics, Drive Systems & Technologies Conference (PEDSTC2015)*. IEEE. 2015, pp. 538–543.

[29] Haolan Shen et al. "Mixed-Type Open-Circuit Fault Diagnosis for NPC Inverters Using a Dual-Input CNN". In: *2021 IEEE 4th International Electrical and Energy Conference (CIEEC)*. IEEE. 2021, pp. 1–7.

[30] Vikram Singh, Anamika Yadav, and Shubhrata Gupta. "Open circuit fault diagnosis and fault classification in multi-level inverter using fuzzy inference system". In: *SJEE* 20.2 (2023), pp. 163–189.

[31] A Sivapriya et al. "Real-time hardware-in-loop based open circuit fault diagnosis and fault tolerant control approach for cascaded multilevel inverter using artificial neural network". In: *Frontiers in Energy Research* 10 (2023), p. 1083662.

[32] Sohaib Tahir et al. "Digital Control Techniques Based on Voltage Source Inverters in Renewable Energy Applications: A Review". In: *Electronics* 7 (Feb. 2018), p. 18. DOI: 10.3390/electronics7020018.

[33] Muhammad Hammad Uddin, Muhammad Baig, and Muhammad Memon. "Comparision of 'perturb observe' and 'incremental conductance', maximum power point tracking algorithms on real environmental conditions". In: Apr. 2016.

[34] Bandaru Urmila and D Subbarayudu. "Harmonic Orientation of Pulse Width Modulation Technique in Multilevel Inverters". In: *Advances in Electrical and Electronic Engineering* 9 (Mar. 2011). DOI: 10.15598/aeee.v9i1.37.

[35] Meng-Hui Wang and Mu-Jia Chen. "Two-Stage Fault Diagnosis Method Based on the Extension Theory for PV Power Systems". In: *International Journal of Photoenergy* 2012 (June 2012). DOI: 10.1155/2012/892690.

[36] Hayder Yousif and Zahraa Al-Milaji. "Fault detection from PV images using hybrid deep learning model". In: *Solar Energy* 267 (2024), p. 112207.